IITRI PROJECT D6087
First Annual Report

THEORETICAL STUDY OF PRODUCTION OF UNIQUE GLASSES IN SPACE

Prepared for:

National Aeronautics and Space Administration
Marshall Space Flight Center, Ala. 35812

ATTENTION: R. L. Nichols

IIT RESEARCH INSTITUTE

IIT RESEARCH INSTITUTE
Ceramics Research
10 West 35th Street
Chicago, Illinois 60616

THEORETICAL STUDY OF PRODUCTION OF UNIQUE GLASSES IN SPACE

FIRST ANNUAL REPORT
1 July, 1973 - 31 June, 1974

Contract No. NAS8-29850
IITRI Project No. D6087

July 23, 1974

Prepared by:
D. C. Larsen

Prepared for:

National Aeronautics and Space Administration
George C. Marshall Space Flight Center
Alabama 35812

TABLE OF CONTENTS

LIST OF FIGURES (Cont'd)

LIST OF TABLES

THEORETICAL STUDY OF PRODUCTION OF UNIQUE GLASSES IN SPACE

1.0 INTRODUCTION AND SUMMARY

The overall objective of this program is to develop analytical functional relationships describing homogeneous nucleation and crystallization in various supercooled liquids. The time and temperature dependent relationships of nucleation and crystallization (intrinsic properties) are being used to relate glass forming tendency to extrinsic parameters such as cooling rate through computer simulation. Single oxide systems are being studied initially to aid in developing workable kinetic models and to indicate the primary materials parameters affecting glass formation. The theory and analytical expressions developed for simple systems is then extended to complex oxide systems. A thorough understanding of nucleation and crystallization kinetics of glass forming systems provides a priori knowledge of the ability of a given system to form a glass. This will facilitate the development of improved glasses by providing a firm theoretical/analytical basis for improved manufacturing techniques such as in-space manufacture. The ultimate objective of space manufacture is to produce technically significant glasses by extending the Earth-limited regions of glass formation for certain compositions, or by achieving glass formation in other compositions that are not glass formers based on empirical Earth observations.

The literature has been reviewed and critically analyzed, and kinetic equations have been developed for homogeneous and heterogeneous nucleation and subsequent crystal growth. The kinetic relationships have been applied to known glass formers and non-glass formers. It was found that the models qualitatively predict earth-observed behavior for these systems. We can now proceed to apply the functional relationships to more complex materials with the goal of utilizing the in-space environment in producing technically improved glasses.

2.0 TECHNICAL DISCUSSION

The concept of glass forming tendency derives from the definition of glass. Morey(1) has defined glass as an inorganic substance in a condition which is continuous with, and analogous to, the liquid state of that substance; but which, as a result of having been cooled from a fused condition, has attained so high a degree of viscosity as to be for all practical purposes rigid. Hence, glass-forming materials are ones in which there is sufficient transient bonding in the melt to produce a highly viscous liquid upon cooling. In the general sense, Morey's restriction of glasses to only inorganic materials can be relaxed to include organic materials as well. The supercooled amorphous state of aggregation of matter comprising a glass is unstable relative to the solid crystalline state. Therefore, glass forming tendency is related to the mechanisms and parameters that prevent the liquid-solid transformation from occurring. Studies of the crystalline transformation can be approached from structural, thermodynamic, and kinetic viewpoints. We have chosen to adopt a kinetic viewpoint since in general glass formation is not related to whether or not a given material can form a glass, but rather how fast must the liquid be cooled from its fused condition to do so.

Therefore, we consider a material to be a glass if it can be cooled from its liquid state rapidly enough to avoid a certain predetermined degree of crystallization. The kinetics of crystallization of a liquid are determined by two parameters, the nucleation rate and the crystal growth rate. The liquid-solid transformation occurs by a two-step process of nucleation of crystalline embryos and subsequent growth. Nucleation and growth rate temperature dependence are illustrated qualitatively in Figure 1. Temperature $T_l = T_m$ is the thermodynamic fusion temperature where the solid and liquid phases are in co-existence. Above T_m the material is in the liquid phase. As the liquid is supercooled below T_m, growth can theoretically occur between temperatures

Figure 1 NUCLEATION AND GROWTH RATE OF CRYSTALS IN GLASS AS FUNCTION OF TEMPERATURE

T_m^- and T_3. However, the embryo nucleation that is necessary before growth can proceed only occurs between temperatures T_2 and T_4. In the temperature region bounded by T_2 and T_3 nucleation and growth occur simultaneously, i.e., conditions are favorable for the complete crystallization transformation process, nucleation and growth. Therefore, the (T_2 - T_3) temperature region is most critical to the prediction of glass formation.

The present program deals with characterizing the nucleation and growth characteristics of several materials, and presentation in a form similar to Figure 1. With the analytical relationships describing nucleation and crystal growth, computer-simulated melt-quench experiments provide information regarding the cooling rates necessary for glass formation (i.e., cooling rates necessary to pass through the (T_2 - T_3) temperature region rapidly enough to prevent crystallization).

The kinetic treatment of glass formation necessarily starts with derivations of nucleation and growth expressions. In the following sections these parameters are discussed in some detail. Succeeding sections will deal with the volume fraction transformed and critical cooling rates, initial computer-modeled results, and a discussion of the problems in predicting the behavior of complex multi-component materials.

3.0 KINETICS OF GLASS FORMATION

Equations describing the kinetics of homogeneous nucleation are developed in this section with allowance for transient effects. The effect of the presence of nucleating heterogeneities are also discussed. Models for subsequent crystal growth are presented. Finally, the method of relating the volume fraction of material transformed to the crystalline state to applied cooling rate through computer simulation is discussed.

3.1 Theory of Homogeneous Steady State Nucleation

A supercooled liquid is a metastable phase relative to the solid phase as indicated by free energy considerations. The liquid system below the fusion temperature T_m tends toward thermodynamic stability by lowering its free energy through the crystalline transformation. The existence of a supercooled liquid phase below T_m (i.e., a glass) is the consequence of 1) a surface energy barrier between the solid and liquid state, and 2) the kinetically inhibited movement of molecules that prevents arrangement in an ordered system (i.e., crystalline phase).

The process initiates as statistical molecular density fluctuations causing clustering of molecules or atoms. The clusters are called nuclei, embryo particles of solid crystalline (transformed) material (transformation to the solid crystalline phase can be considered merely as molecular rearrangement into an ordered structure). In tending toward thermodynamic stability there is a volume free energy decrease as an embryo is created (i.e., in the transformation from liquid to crystalline). However, the formation of an embryo means the formation of a boundary, the embryo-liquid interface, with a resulting system free energy gain due to the interfacial surface energy. Jackson (2) discusses the stability of such a nucleus in an undercooled liquid with respect to these two phenomena. For small embryos the surface area is large relative to the volume, so that the surface energy dominates embryo behavior. Small embryo can decrease the total free energy of the system (liquid and nuclei) by shrinking to reduce their surface area (i.e., dissolving into the liquid melt).

Larger size crystalline embryos are controlled by the volume free energy term. Large nuclei can reduce the total free energy of the system by growing larger, creating more transformed crystalline material (more ordered, more stable). A balance between these tendencies defines the critical size nucleus. A nucleated embryo smaller than the critical size will dissolve. A nucleated embryo larger than the critical size will continue to grow.

Consider a liquid melt at temperature T with order fluctuations. This system can be described as a steady state concentration of ordered regions (crystalline in structure) of various sizes. The change in free energy of the system, ΔF, due to a local fluctuation creating a spherical nucleus may be expressed:

$$\Delta F = -\frac{4}{3}\pi r^3 \Delta f_v + 4\pi r^2 \Delta f_s \qquad (1)$$

where r = embryo radius

Δf_v = free energy difference between the liquid and solid state, per unit volume

Δf_s = interfacial (surface) free energy between the phases, per unit area.

The system free energy change has a maximum value, ΔF^*, for some critical nucleus radius, r^*. The critical nucleus size, r^*, represents the smallest size embryo that can grow with a decrease in free energy to form stable nuclei. The critical nucleus size is derived as follows. Differentiating ΔF with respect to r gives

$$\frac{\partial \Delta F}{\partial r} = -4\pi r^2 \Delta f_v + 8\pi r \Delta f_s \qquad (2)$$

Expression (1) has a maximum, ΔF^*, for a value of $r = r^*$ satisfying

$$\frac{\partial \Delta F}{\partial r} = 0 \qquad (3)$$

Setting the r.h.s. of expression (2) equal to zero and solving for $r = r^*$ we obtain

$$r^* = \frac{2\Delta f_s}{\Delta f_v} \qquad (4)$$

Evaluating the expression for ΔF (Equation (1)) for $r = r^*$ yields ΔF^*, the minimum work required to form a stable nucleus:

$$\Delta F^* = \frac{16\pi}{3} \frac{\Delta f_s^{\,3}}{\Delta f_v^{\,2}} \qquad (5)$$

The term ΔF^* is the thermodynamic barrier to the nucleation process of forming stable nuclei. We now turn our attention to obtaining the surface and volume terms in ΔF^* in more useful form.

Turnbull (3) has shown that the liquid-crystal surface tension, Δf_s, can be related to the heat of fusion, Δh_f, by the expression

$$\Delta f_s = \frac{\Delta h_f}{\alpha} N^{-1/3} V_m^{-2/3} \qquad (6)$$

where Δh_f = molar latent heat of fusion of the crystalline phase (cal mole^{-1})

N = Avagadro's number ($\sim 6\times10^{23}$ molecules mole^{-1})

V_m = molar volume of the crystalline phase (cc/mole)

The dimensionless term α relates the proportionality of Δh_f and Δf_s, and is constant for a given type of fluid (3). For metals $\alpha \backsim 2$, for more complex materials $\alpha \backsim 3.3$. Therefore, α has an approximate range

$$2 \leq \alpha \leq 3.3 \qquad (7)$$

The parameter α is defined such that physically the recipricol of α, $1/\alpha$, is equal to the number of monolayers per unit area of crystal which would be melted at T_m by an enthalpy $\Delta H = \Delta f_s$.

The volume free energy difference between the liquid and solid states, Δf_v, is expressed:

$$\Delta f_v = \int_{T_m}^{T} \left(\frac{\Delta s_f}{V_m} \right) dT \qquad (8)$$

which is estimated for small supercooling $\Delta T = T_m - T$:

$$\Delta f_v = \frac{\Delta s_f \Delta T}{V_m} \qquad (9)$$

where Δs_f is the molecular entropy of fusion (cal $mole^{-1} deg^{-1}$). Since the entropy of fusion is related to the heat of fusion, Δh_f (cal/mole)

$$\Delta s_f = \frac{\Delta h_f}{T_m} \qquad (10)$$

the expression for Δf_v (per unit volume) can be expressed

$$\Delta f_v = \frac{\Delta h_f}{T_m} \frac{\Delta T}{V_m} \qquad (11)$$

At large degrees of undercooling $\Delta T = T_m - T$, this expression is modified by the factor T/T_m

$$\Delta f_v \text{ (large } \Delta T) = \frac{\Delta h_f}{T_m} \frac{\Delta T}{V_m} \left(\frac{T}{T_m} \right) \qquad (12)$$

Limiting our analysis to the case of small undercooling, use of Equations (6) and (11) for Δf_s and Δf_v, respectively, permits expression of r* from Equation (4) in more useful terms:

$$r^* = \frac{2 T_m V_m^{1/3}}{\alpha N^{1/3} \Delta T} \qquad (13)$$

For clusters(embryo) below T_m with radius $r < r^*$, nuclei form and dissolve because the surface energy involved in cluster formation is greater than the free energy change accompanying solid formation. For $r > r^*$, continuous nuclei growth will occur since the surface energy is growing only proportional to r^2 while the bulk (volume) free energy term involved in solid formation is growing proportional to r^3. Above T_m crystalline

embryo are unstable. Critical cluster radii are illustrated in Figure 2 for various oxide systems.

The thermodynamic barrier to nucleation, ΔF^*, is expressed in more useful terms, employing Equation (6) and (11) for Δf_s and Δf_v respectively:

$$\Delta F^* = \frac{16\pi}{3} \frac{\Delta h_f^2 T_m^2}{\alpha^3 N \Delta T^2} \tag{14}$$

It will be convenient to express ΔF^* in terms of another dimensionless parameter, β, defined (9) such that

$$\Delta s_f = Nk\beta = R\beta \tag{15}$$

where k = Boltzmann's constant.

R = 1.987 cal $mole^{-1} deg^{-1}$ = gas constant

The heat of fusion, Δh_f, thus becomes

$$\Delta h_f = \Delta s_f T_m = R\beta T_m = Nk\beta T_m \tag{16}$$

The parameter β has range

$$1 \leq \beta \leq 10 \tag{17}$$

with $\beta = 1$ for monatomic liquids. More complex structures have higher entropies of fusion, with β approaching $\beta = 10$.

The expression for ΔF^* (Equation 14) is expressed in terms of β:

$$\Delta F^* = \frac{16\pi}{3} \frac{k\beta T_m^3}{\alpha^3 \Delta T^2} \tag{18}$$

Having developed an expression based on thermodynamics and free energy considerations for the minimum work required for homogeneous nucleation (i.e., the thermodynamic barrier to nucleation), we must now derive an expression for the rate of homogeneous nucleation. If it is assumed that critical size clusters ($r = r^*$) are formed by statistical molecular fluctuations the nucleation rate will be proportional to a term involving the probability of such a fluctuation, exp ($-\Delta F^*/kT$). The steady state nucleation rate involving a Boltzmann-like distribution of critical size nuclei is expressed:

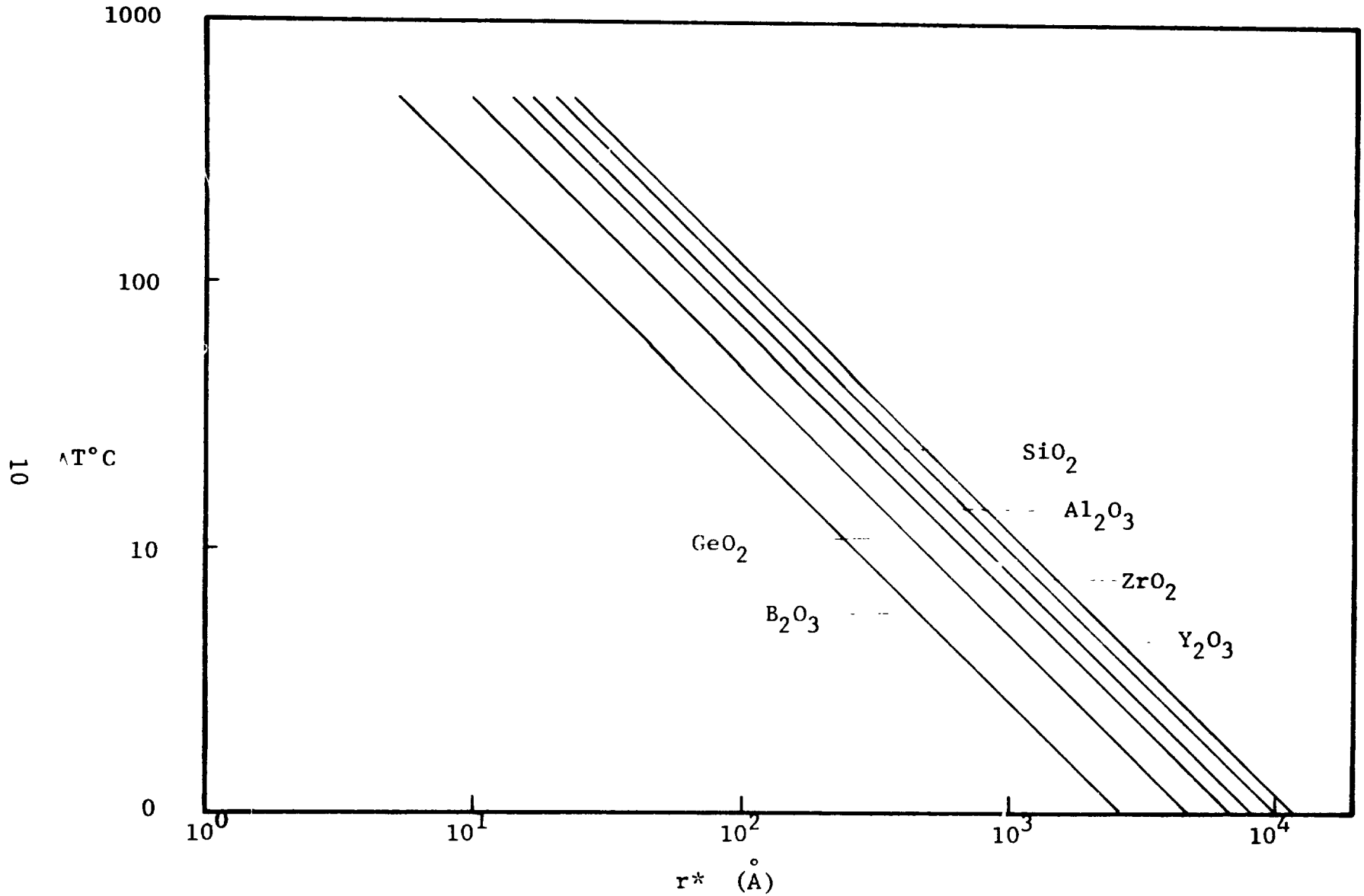

Figure 2 RADII r* OF CRITICAL EMBRYOS AS FUNCTION OF UNDERCOOLING ΔT FOR VARIOUS OXIDES (α = 2)

$$I_o = n\nu_n \exp(-\Delta F^*/kT) \qquad (19)$$

where n = number of molecules per unit volume in the system ($n = \frac{N}{V_m} \sim 10^{22}$) and ν_n is a molecular attempt frequency for nucleation.

This result is derived from thermodynamics and thermostatistics. However, the nucleation process involves molecular movement. Therefore, a kinetic or diffusional barrier also exists for the nucleation process. The steady state nucleation rate, I_o (nuclei $cc^{-1}sec^{-1}$), is expressed in general terms

$$I_o = n\nu_n \exp(-\Delta F^*/kT)\exp(-\Delta G'/kT) \qquad (20)$$

where $\Delta G'$ is the activation energy for molecular motion (during nucleation) across the embryo-matrix interface. Thus the nucleation rate (steady state) is a function of (1) the number of molecular or atomistic units available for nucleation, (2) a frequency factor describing how often the molecules attempt to jump across the liquid-nucleus boundary, (3) a thermodynamic barrier to nucleation, the minimum work required to form a stable nucleus, and (4) a kinetic barrier to nucleation, involving the activation energy for molecular rearrangement.

If the molecular motion involved in nucleation is treated as an activated process (4), a diffusional rate constant for nucleation, D_n, can be defined such that

$$D_n = a_o^2 \nu_n \exp(-\Delta G'/kT) \qquad (21)$$

where a_o is the molecular jump distance.

Combining Equations (20) and (21) yields the following expression for the steady state nucleation rate:

$$I_o = \frac{nD_n}{a_o^2} \exp(-\Delta F^*/kT) \qquad (22)$$

The problem now arises as how to evaluate the nucleation diffusional rate constant, D_n. For liquids which crystallize without change in composition (single component systems, for instance) long range diffusion processes are not required. All of the atomic or molecular units required for the ordered crystalline structure are in the local vicinity of the liquid-crystal interface. This type of transformation is termed non-reconstructive. The activation energy, $\Delta G'$, for diffusion at the liquid-crystal interface will be roughly the same order of magnitude as the activation energy for viscous flow. This is the case for a liquid transforming to solid without change in composition since the movements of the atoms or structural units on the nucleation surface is similar to the reorientation of structural units and bond switching in the flow of a viscous liquid. Therefore, in this simple case, the nucleation diffusional rate constant, D_n, will be approximately equal to the self diffusion coefficient of the undercooled liquid:

$$D_n \backsim D_s \tag{23}$$

The liquid self diffusion coefficient, D_s, is related to the bulk viscosity, η, through the Stokes-Einstein relation

$$D_s = \frac{kT}{3\pi a_o \eta} \tag{24}$$

where a_o is the diameter of the diffusing species.

Therefore, for the case of a single component substance, or a more complex liquid that crystallizes with no change in composition, the steady state nucleation rate is expressed (for small degrees of undercooling below T_m)

$$I_o = \frac{nkT}{3\pi a_o^3 \eta} \exp\left[\frac{-16\pi \beta T_m^3}{3 \alpha^3 T \Delta T^2}\right] \tag{25}$$

where all terms have been previously defined.

The general temperature dependence of the homogeneous

nucleation rate described by Equation 25 is shown in Figure 1. For small degrees of undercooling below T_m, ΔF^*, the thermodynamic barrier, is large since Δf_v, the volume free energy change in the transformation is small. This results in low nucleation rates. With further supercooling Δf_v increases until $\Delta F^* \backsim \Delta G'$, the kinetic barrier to nucleation. This condition results in maximum nucleation rate. For a large ΔT the nucleation rate decreases to a negligible level as $\Delta G' > > \Delta F^*$.

In the case where a compositional change accompanies the liquid-solid transformation, the steady state nucleation rate (Equation 25) must be modified to account for the long range diffusion processes that are required for molecular rearrangement. This subject will be treated in Section 6.0.

3.1.1 Time-Dependent Homogeneous Nucleation

In this discussion transient effects on nucleation are considered. Glass forming tendency is related to how fast the system can pass through the region of simultaneous nucleation and growth (i.e., the (T_2-T_3) region shown in Figure 1). The time spent at any particular temperature level may then be less than the time required to establish a steady nucleation rate (i.e., the time required to build up the required Boltzmann-like distribution of embryos).

Incorporation of time-dependence into nucleation theory has been treated by Hillig (5) and Hammel (4), and takes the form

$$I_t = I_o e^{-\tau/t} \qquad (26)$$

where I_t = transient nucleation rate
I_o = steady state nucleation rate
t = time

Hammel(4) has expressed the parameter τ (after Collins(6)) as:

$$\tau = \frac{144kTT_mV_m^{1/3}}{N^{1/3}\alpha a_o^2 \Delta s_f \Delta T^2 D} \qquad (27)$$

where D is the appropriate diffusion coefficient (given by the Stokes-Einstein Equation for transformation without change of composition) and all other terms have been previously defined. This equation was derived for the ideal case of instantaneous cooling from T_m to T.

Hillig (5) derived an approximate expression for τ using random walk diffusion theory to describe the mean time $\bar{t}$ to build a critical nucleus:

$$\tau = \bar{t} = \frac{\pi V_L^2 r^{*2}}{4DV_m^2 X^2} \qquad (28)$$

where V_L and V_m are the mole volumes of the liquid and precipitating phase, respectively, D is again the appropriate diffusion coefficient ($D = D_s$ for crystallization without change in composition), and X is the mole fraction of the precipitating phase in the liquid (i.e., X = 1 for crystallization without change in composition).

Hillig's $\bar{t}$ parameter has been shown (4) to more accurately describe time-dependence of the nucleation rate, based on correlation with experimental results. Therefore, we shall employ Equations (26) and (28) when simulating nucleation in computer generated melt-quench experiments.

The nature of transient effects on nucleation rate is illustrated qualitatively in Figure 3. Due to diffusional effects successively longer times are required to achieve steady state nucleation at successively lower temperatures. If the hypothetical material whose nucleation characteristics are shown in Figure 3 is cooled from T_m to T_1, detectable nucleation would be avoided at any cooling rate.* However, a detectable level of homogeneous nucleation occurs between temperatures T_1 and T_2. In order to avoid this nucleation in a melt-quenching experiment the temperature region T_1 - T_2 must be passed through in less than time t_2.

* For many materials $T_1/T_m \backsim .8$

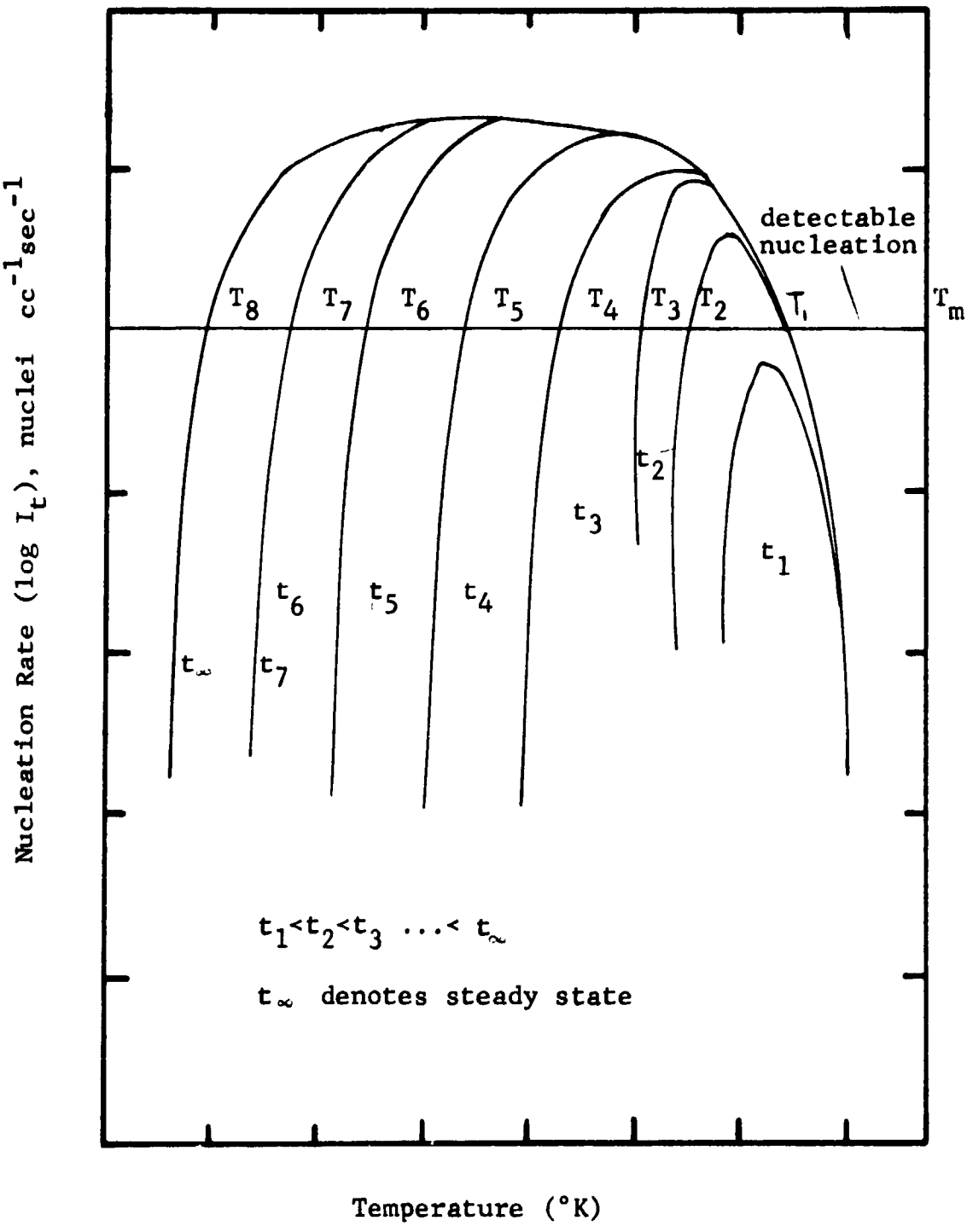

Figure 3 NUCLEATION RATE SHOWING TRANSIENT EFFECT

If this glass were successfully quenched to temperature T_6, for instance, it could be held at this temperature level for a period of time t_6 before detectable nucleation would occur (e.g., for annealing).

As shall be discussed in Section 6.0, the transient nucleation formulation provides one possible way of dealing with multicomponent systems where long range diffusion processes are required for molecular rearrangement.

3.2 Heterogeneous Nucleation

Thus far we have only treated the case of homogeneous nucleation in pure substances free of impurities, insoluble particles, etc. Foreign surfaces present in the liquid, such as container walls or insoluble particles, however, tend to reduce the barrier to nucleation represented by the surface energy between the liquid and solid phases. As a result the critical embryo size is reduced and the "supercooling temperature" is raised. The "supercooling temperature" is the temperature T_2 where the first detectable nucleation is observed upon cooling from the melt. This effect is shown qualitatively in Figure 4.

At heterogeneous surface sites the computation of the critical embryo size becomes complicated because of the various surface energies involved and the particular geometry of the embryo surface. Furthermore, the wettability of the foreign surface by the liquid must be taken into account.

For our present purposes we shall only treat the effect of heterogeneous nucleation qualitatively, following the treatment of several authors (references 2,4,5,7-9) in order to illustrate the nature of the analytical expressions.

The work term for heterogeneous nucleation, ΔF^*_θ, is given generally as

$$\Delta F^*_\theta = f(\theta) \cdot \Delta F^* \qquad (29)$$

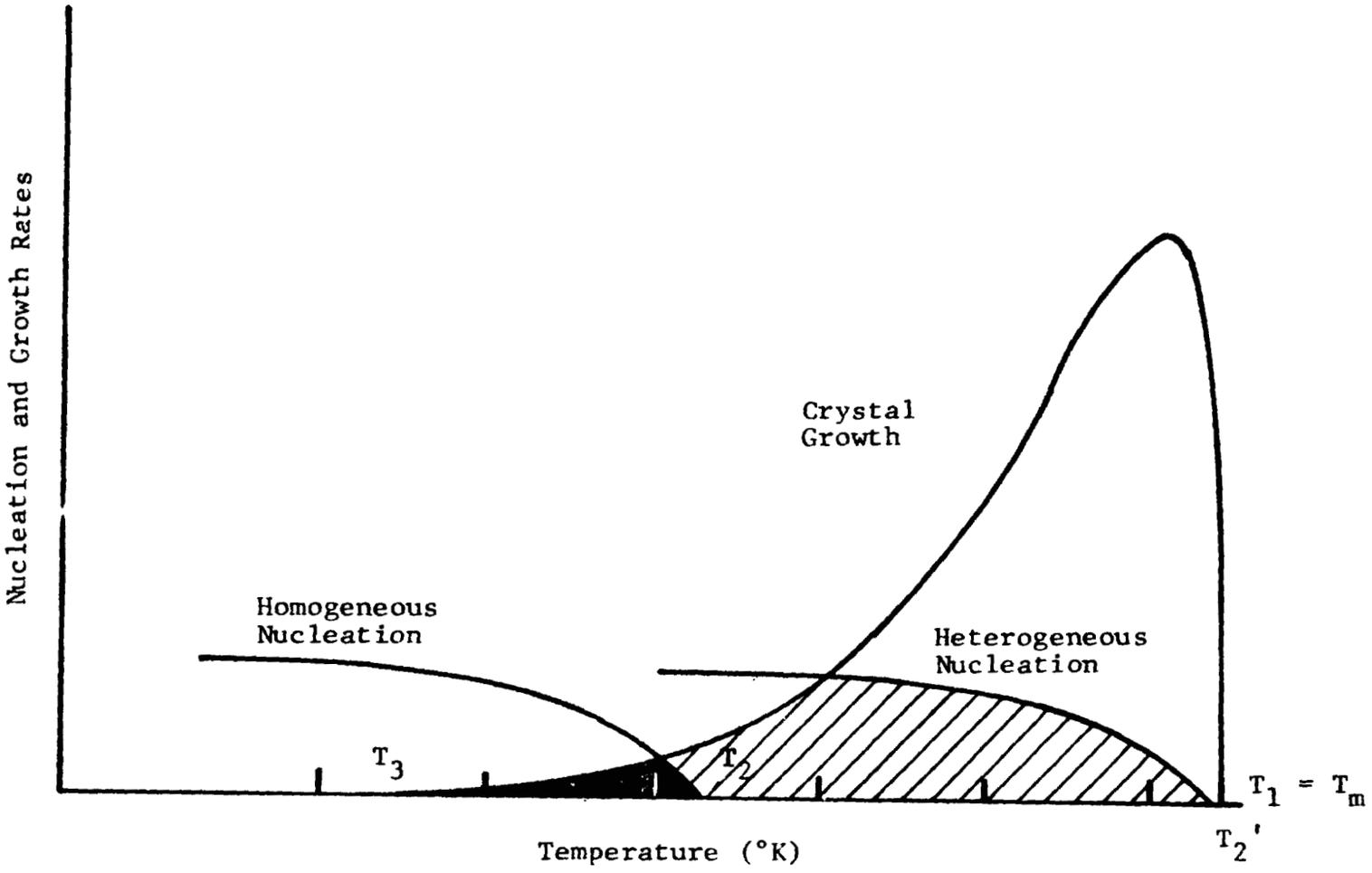

Figure 4 EFFECT OF HETEROGENEOUS NUCLEATION ON GLASS FORMING TENDENCY

where the factor $f(\theta)$ is expressed

$$f(\theta) = \frac{(2 + \cos\theta)(1 - \cos\theta)^2}{4} \qquad (30)$$

The angle θ is a function of the balance of surface tensions and is given by:

$$\cos\theta = \frac{\sigma_{sL} - \sigma_{s\beta}}{\sigma_{L\beta}} \qquad (31)$$

where σ_{sL}, $\sigma_{s\beta}$ and $\sigma_{L\beta}$ are the interfacial energies between the solid-liquid, solid-impurity surface, and the liquid-impurity surface, respectively.

The lowering of the net interfacial energy in heterogeneous nucleation depends on how well the impurity surface wets the nucleating phase in the presence of the liquid.

Therefore, if heterogeneous nucleation sites are present the minimum work required (thermodynamic barrier to nucleation) to form a stable nucleus is reduced. The treatment is further complicated by the fact that the concentration of nuclei deriving from a heterogeneous mechanism will be some function of the concentration of impurity sites present, and not given simply by a nucleation rate formulation.

3.3 Crystal Growth Kinetics

Once formed by a homogeneous or heterogeneous nucleation mechanism, stable nuclei will continue to grow at a rate determined primarily by the rate at which the atoms necessary for growth can diffuse to the surface of the crystal, and by the ease with which they can free themselves from the attractions of their neighbors in the liquid phase and form new bonds in the specific positions determined by the structure of the growing crystal (10). The fundamental concept here is that growth is considered in terms of molecular rearrangement.

Crystal growth is either interface-controlled or diffusion-controlled. Interface-controlled growth occurs when the rate controlling step occurs at the liquid-crystal interface.

This normally occurs for single component glasses, for instance, where only short range molecular rearrangement at the liquid-crystal interface is necessary. Diffusion-controlled growth occurs when the rate controlling step is the long range diffusion of a given species in the bulk liquid. Thus, diffusion-controlled growth would normally apply in the case where crystallization is accompanied by a large change in composition, such as for complex multicomponent systems.

3.3.1 Interface-Controlled Growth Kinetics

For this work we shall restrict ourselves to the case of crystallization without change in composition as we have done for the case of homogeneous nucleation in the preceding sections. Thus, we will treat in this section only the mechanisms and kinetics of interface-controlled growth.

Two basic mechanisms have been proposed for interface-controlled growth: continuous growth and lateral growth (11). In continuous growth the crystal interface advances by molecular incorporation which can occur with equal probability everywhere (except for certain anisotropic effects). Lateral growth occurs either by a two-dimensional nucleation mechanism or by a screw dislocation spiral growth ramp mechanism depending on the crystal perfection.

In systems which crystallize without change in composition the nature of the liquid-crystal interface strongly influences the kinetics and morphology of crystallization. Different models for interface controlled growth are each based on a different assumption concerning the interface and the nature of the sites on the interface where atoms are added or removed. Again, it is important to think of crystal growth as merely a molecular rearrangement process.

The general form of the growth velocity for all interface-controlled growth processes is:

$$\mu = f a_o \nu_g \exp(-\Delta G''/RT) \left[1 - \exp(-\Delta G/RT) \right] \quad (32)$$

where: f = fraction of preferred growth sites on the interface (i.e., fraction of sites available for growth, $0 < f \leq 1$).

ν_g = frequency factor for molecular transport at the liquid-crystal interface (during growth).

a_o = distance advanced by the interface in a unit kinetic process ($\sim$ molecular diameter).

ΔG = free energy change accompanying the liquid-crystal transformation

$\Delta G''$ = free energy of activation or kinetic barrier for the movement of an atom across the liquid-crystal interface during crystallization (i.e., growth).

The kinetic term $\Delta G''$ involved in growth is not necessarily equal to (or even the same order of magnitude) as the kinetic term involved in nucleation, $\Delta G'$ (Equation (20)). Growth may be governed by atomic movements from a great distance away from the liquid-crystal interface. Nucleation (initiation of the transformation) is governed by atomic movement relatively close to the developing nucleus.

Assuming that we can treat the molecular movements involved in crystal growth as simply activated processes, we can define a diffusion coefficient, or rate constant, for the molecular rearrangement

$$D_g = a_o^2 \nu_g \exp(-\Delta G''/RT) \quad (33)$$

in a manner similar to the case of nucleation described in Section 3.1. The general interface-controlled growth expression (Equation (32)) thus becomes:

$$\mu = \frac{f D_g}{a_o} \left[1 - \exp(-\Delta G/RT) \right] \quad (34)$$

Experience on a variety of pure substances which crystallize without change in composition has indicated that the slow, rate controlling step in the interface growth process is the same molecular process that occurs in the bulk liquid above the thermodynamic fusion temperature, T_m(3). Therefore, in this most straightforward of cases, the rate constant for interface-controlled growth, D_g, will have approximately the same value as the liquid self diffusion coefficient, D_s, and thus be approximated by the Stokes-Einstein relation:

$$D_g \approx D_s = \frac{kT}{3\pi a_o \eta} \tag{35}$$

The free energy change accompanying the liquid-crystal transformation, ΔG, is given by

$$\Delta G = \Delta s_f \Delta T \tag{36}$$

The growth velocity for interface-controlled growth without composition change is thus expressed

$$u = \frac{fkT}{3\pi a_o^2 \eta}\left[1 - \exp\left(\frac{-\Delta s_f \Delta T}{RT}\right)\right] \tag{37}$$

or in terms of the β parameter ($\Delta s_f = Nk\beta = R\beta$)

$$u = \frac{fKT}{3\pi a_o^2 \eta}\left[1 - \exp\left(\frac{-\beta \Delta T}{T}\right)\right] \tag{38}$$

since

$$R = Nk \tag{39}$$

We will now briefly treat the various models that have been proposed for interface-controlled growth. The models and discussion presented have been taken from Uhlmann (12).

3.3.1.1 Normal (Continuous) Growth

In normal or continuous growth atoms can attach to or be removed from any site on the interface. Thus, there are no preferred growth sites in the interface, and f in Equation (37) becomes unity.

$$\mu = \frac{kT}{3\pi a_o^2 \eta} \left[1 - \exp\left(\frac{-\Delta s_f \Delta T}{RT}\right)\right] \qquad (40)$$

For small departures from equilibrium, this model predicts a linear relation between growth rate, μ, and undercooling, ΔT. For this model to correlate with experimental data the liquid-crystal interface must be rough on an atomic scale.

3.3.1.2 Screw Dislocation Growth

In the screw dislocation model growth occurs at step sites provided by screw dislocations intersecting the interface. The fraction of preferred growth sites, f in Equation (37), is expressed

$$f = \frac{a_o \Delta h_f \Delta T}{4\pi\sigma T_m V_m} \backsim \frac{\Delta T}{2\pi T_m} \qquad (41)$$

where it has been assumed that only molecular transport within a molecular diameter, a_o, of the dislocation ledge results in attachment. For small undercooling, ΔT, this model predicts a growth rate which varies with ΔT^2. For the screw dislocation model to apply, the interface must be smooth on an atomic scale, and be relatively imperfect in the crystallographic sense.

3.3.1.3 Surface Nucleation Growth

According to this model growth takes place at step sites provided by two-dimensional nuclei formed on the interface. The growth rate can be expressed

$$\mu = A\nu \exp(-B/T\Delta T) \qquad (42)$$

where the exponential constant is

$$B = \frac{\pi a_o V_m T_m \sigma_E^2}{k\Delta h_f} \qquad (43)$$

The term σ_E is the specifi edge surface energy of the nucleus. The frequency factor, ν, can be derived from the growth rate

constant:

$$\nu = \frac{D_g}{a_o^2} \qquad (44)$$

The growth velocity predicted by this model should vary exponentially with the undercooling, ΔT, and for small ΔT should be unobservably low. For this model to correspond to experimental observation the interface must be smooth on an atomic scale and be defect-free.

This comment and the foregoing discussions regarding expected morphology for each of interface-controlled growth models will have application in the experimental stages of our NASA program (to be discussed later). For materials which have not been extensively studied, morphological studies (SEM, etc.) will indicate, by inference, which growth model applies to a given material. Utilizing empirical results of melt-quench experiments to correlate with our kinetic relationships will help to indicate how space processing can be utilized to produce glasses unobtainable on Earth.

3.3.2 Significance of Entropy of Fusion

As discussed by Uhlmann (12) growth rates depend critically on the molecular structure of the liquid-crystal interface. The interface structure, in turn, depends significantly on a bulk thermodynamic property, the molecular entropy of fusion, Δs_f.

For materials characterized by low entropies of fusion ($\Delta s_f < 2R$) the liquid-crystal interface should be rough on an atomic scale, defects should not affect growth, and normal growth kinetics are predicted (i.e., Equation (40)). On the scale of light microscopy the crystal-liquid interface should be non-faceted.

For materials characterized by large entropies of fusion ($\Delta s_f > 4R$) faceted interface morphologies should be observed, defects should be important to growth, and the kinetics of the

normal growth model should not apply. Except as limiting cases, the observed growth velocities for large Δs_f materials should not agree well with behavior predicted by screw dislocation model or the surface nucleation model either.

4.0 VOLUME FRACTION TRANSFORMED AND CRITICAL COOLING RATES

Glass forming tendency can quantitatively be described in terms of the volume fraction of crystalline material formed during a certain quenching operation. Uhlmann (13) has expressed the volume fraction, v_f, crystallized in time, t, (for small v_f) as

$$v_f \backsim 1/3\ \pi I\ \mu^3 t^4 \qquad (45)$$

where I = nucleation rate (nuclei $cc^{-1} sec^{-1}$)
μ = growth velocity (cm sec^{-1})
t = time (sec)

This relation is valid for interface-controlled growth, and thus applies to single component or congruently melting (i.e., without change in composition) compounds.

The critical cooling rate for glass formation, i.e., the minimum cooling rate necessary to avoid a certain volume fraction of transformed material, can be estimated by a procedure employed by Uhlmann (13). T-T-T (time-temperature-transformation) curves are constructed as illustrated qualitatively in Figure 5. Using Equation (45), the time required to transform a given amount of material is calculated as a function of temperature. A volume fraction transformed $v_f = 10^{-6}$ is regarded as just-detectable. The data are presented graphically as ΔT vs t in the T-T-T plot. The critical cooling rate can be approximated (13) by the expression

$$\left.\frac{dT}{dt}\right|_{critical} = \frac{\Delta T_N}{\tau_N} \qquad (46)$$

where $\Delta T_N = T_m - T_N$
T_N = temperature at the nose of the T-T-T curve
τ_N = time at the nose of the T-T-T curve

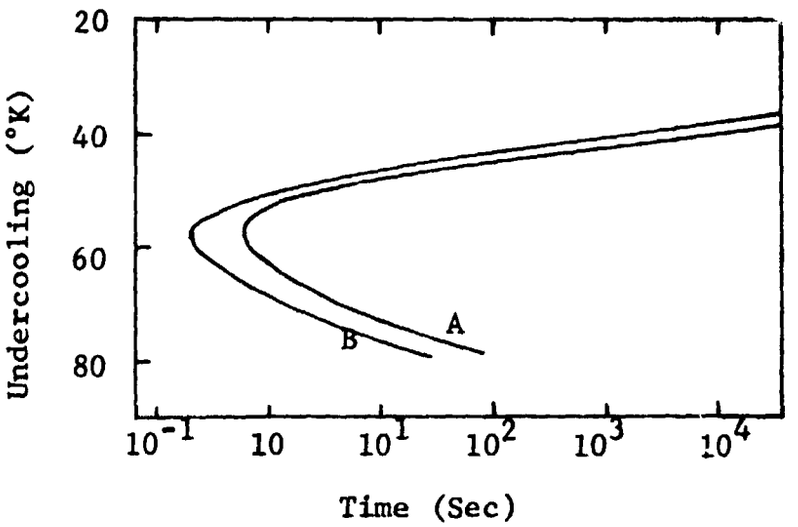

Figure 5 TIME-TEMPERATURE-TRANSFORMATION CURVE (TAKEN FROM UHLMANN (13))

5.0 COMPUTER MODELED RESULTS FOR SELECTED SYSTEMS

The kinetics developed for nucleation and growth are now applied to several materials systems. The well-characterized silica, SiO_2, system is investigated for the purpose of determining the relative importance of the various kinetic and thermodynamic parameters in controlling transformation behavior. The B_2O_3 system is studied to determine if the derived kinetic relationships will predict its good glass forming qualities, and imply a physical reason for the observed behavior. The alumina, Al_2O_3, system is studied to determine if the kinetics can predict the poor glass forming tendency that is observed on earth, and imply a physical reason for this phenomenon.

5.1 The Silica System (SiO_2)

The pertinent materials properties for the silica system to be used in the derived kinetic nucleation and growth expressions are tabulated in Table I. Viscosity data for the silica system are shown in Figure 6, compared with viscosity data for other oxide systems.

These materials parameters were inserted into the derived nucleation and growth kinetics (Equations (25), (26), (28), and (37)), with results illustrated in Figures 7 and 8. The low temperature cut-off in the nucleation rate has been discussed previously. Figure 7 indicates the relative time scale of this effect. A nucleation rate of 1 nuclei $cc^{-1}sec^{-1}$ has arbitrarily (but by popular custom (5)) been taken as the level of detectable nucleation. As illustrated in Figure 7, detectable homogeneous nucleation for SiO_2 does not occur upon cooling from the melt (T_m) until roughly 1700° to 1750°K. Above about 1200°K the thermodynamic barrier to nucleation controls behavior. Below ~ 1200°K the kinetic (diffusional) factor dominates. The peak growth rate for SiO_2 (Figure 8) is roughly 40 Å/min, and occurs at roughly 50°K undercooling below T_m. The crystal growth rate is seen to be zero at T_m, the thermodynamic fusion temperature. For small values of supercooling (temperatures during quench

TABLE I

MATERIALS PARAMETERS FOR SiO_2

Δh_f = 2000 cal $mole^{-1}$

T_m = 2000°K

$\Delta s_f = \frac{\Delta h_f}{T_m}$ = 1 cal $mole^{-1}K^{-1}$

$\beta = \frac{\Delta s_f}{R} \backsim .5$

a_o = 2.5 Å ($\backsim$0-0 distance in SiO_4 tetrahedron)

f = 1 (normal growth assumed)

X = 1 (pure substance)

$V_m = V_L$ = 27.6 cc $mole^{-1}$

η (viscosity): see Figure 6

α = 2.5 (representative value)

N = 6×10^{23} molecules $mole^{-1}$

$n = \frac{N}{V_m}$ = 2×10^{22} molecules cc^{-1}

$\Delta T = T_m - T$

k = Boltzmann's constant = 1.38×10^{-16} erg C^{-1} = 3.3×10^{-24} cal C^{-1}

R = gas constant $\backsim$ 1.987 cal $mole^{-1}deg^{-1}$

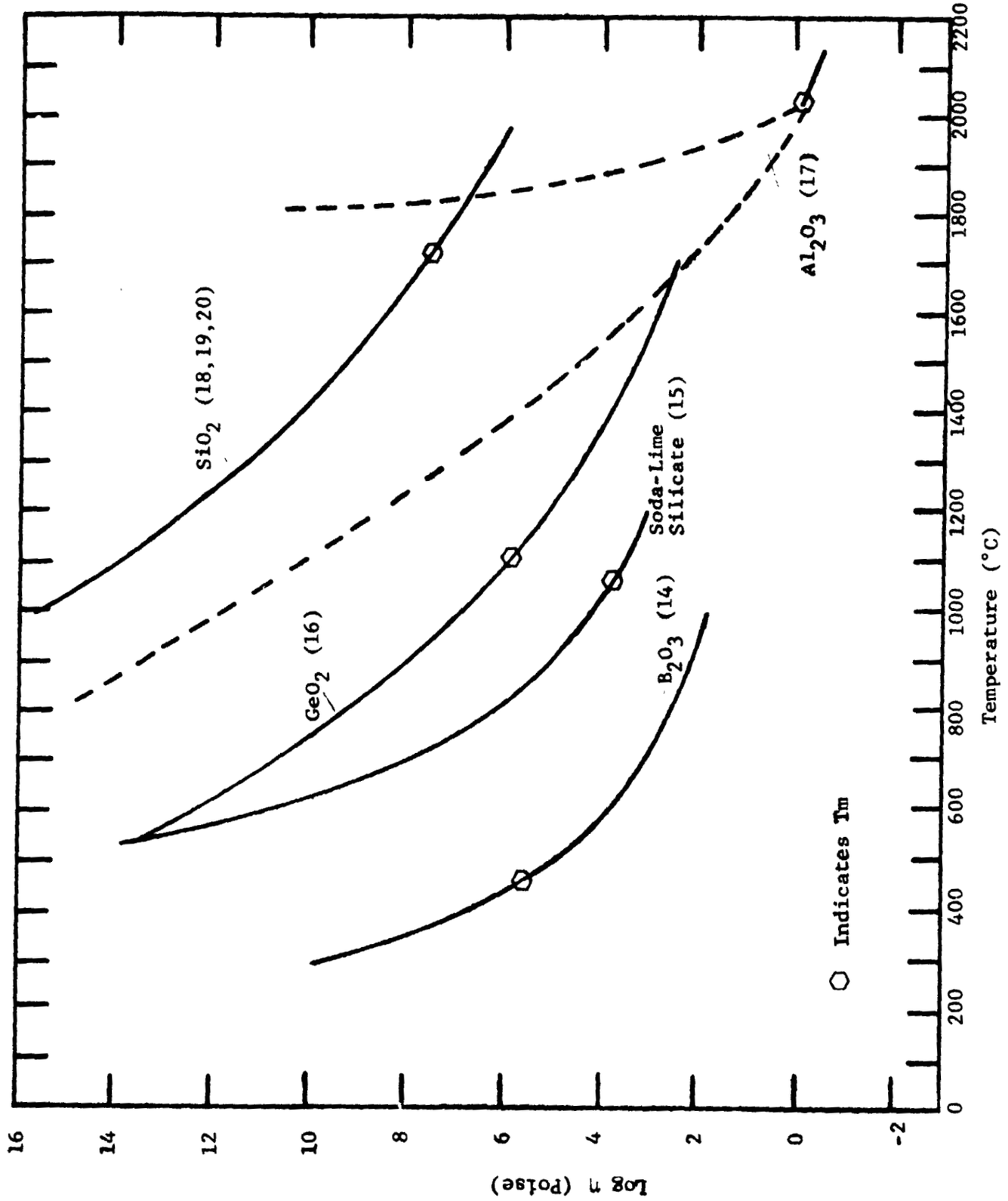

Figure 6 VISCOSITY FOR VARIOUS MATERIALS

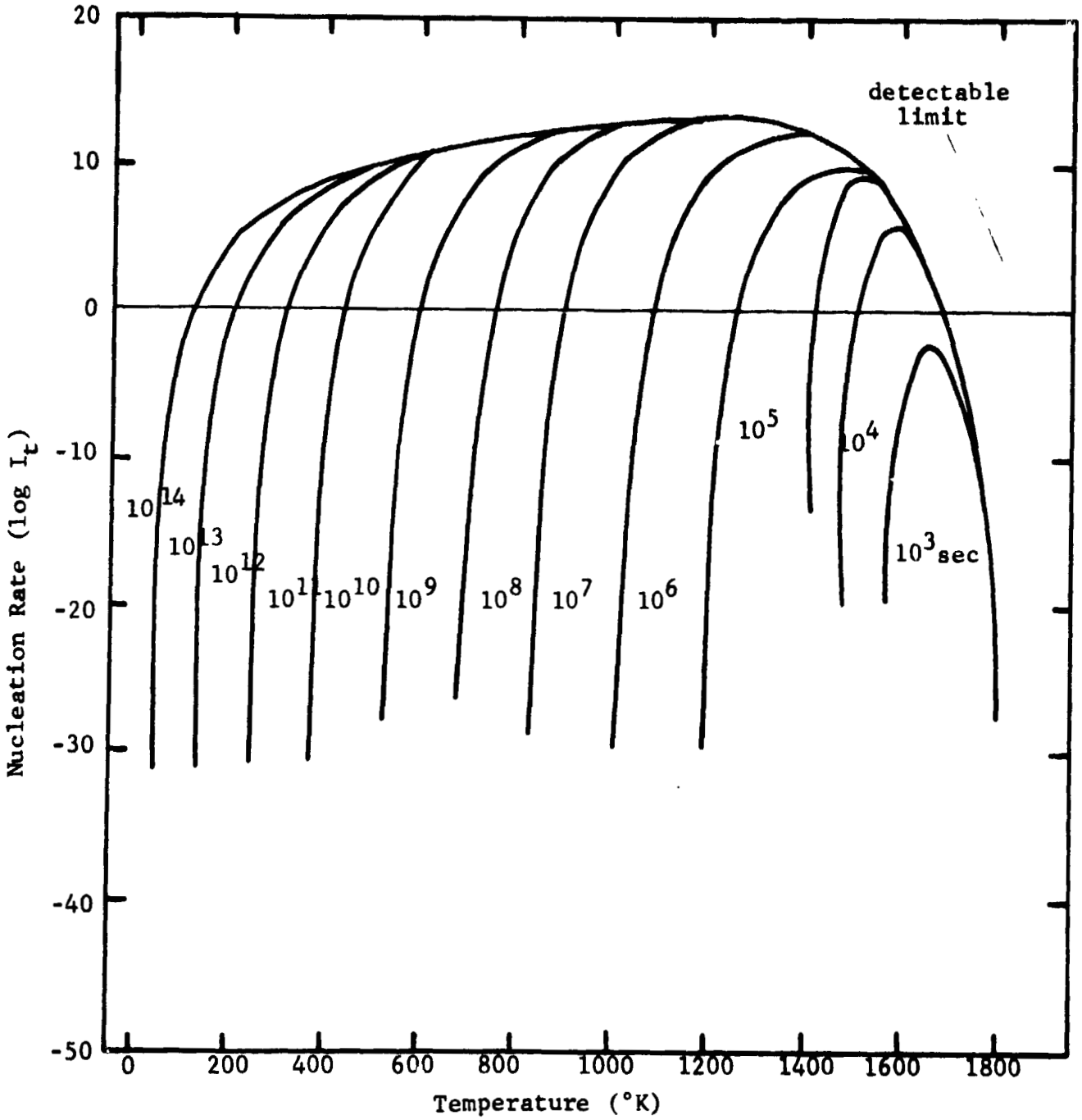

Figure 7 NUCLEATION RATE SHOWING TRANSIENT EFFECT FOR SILICA

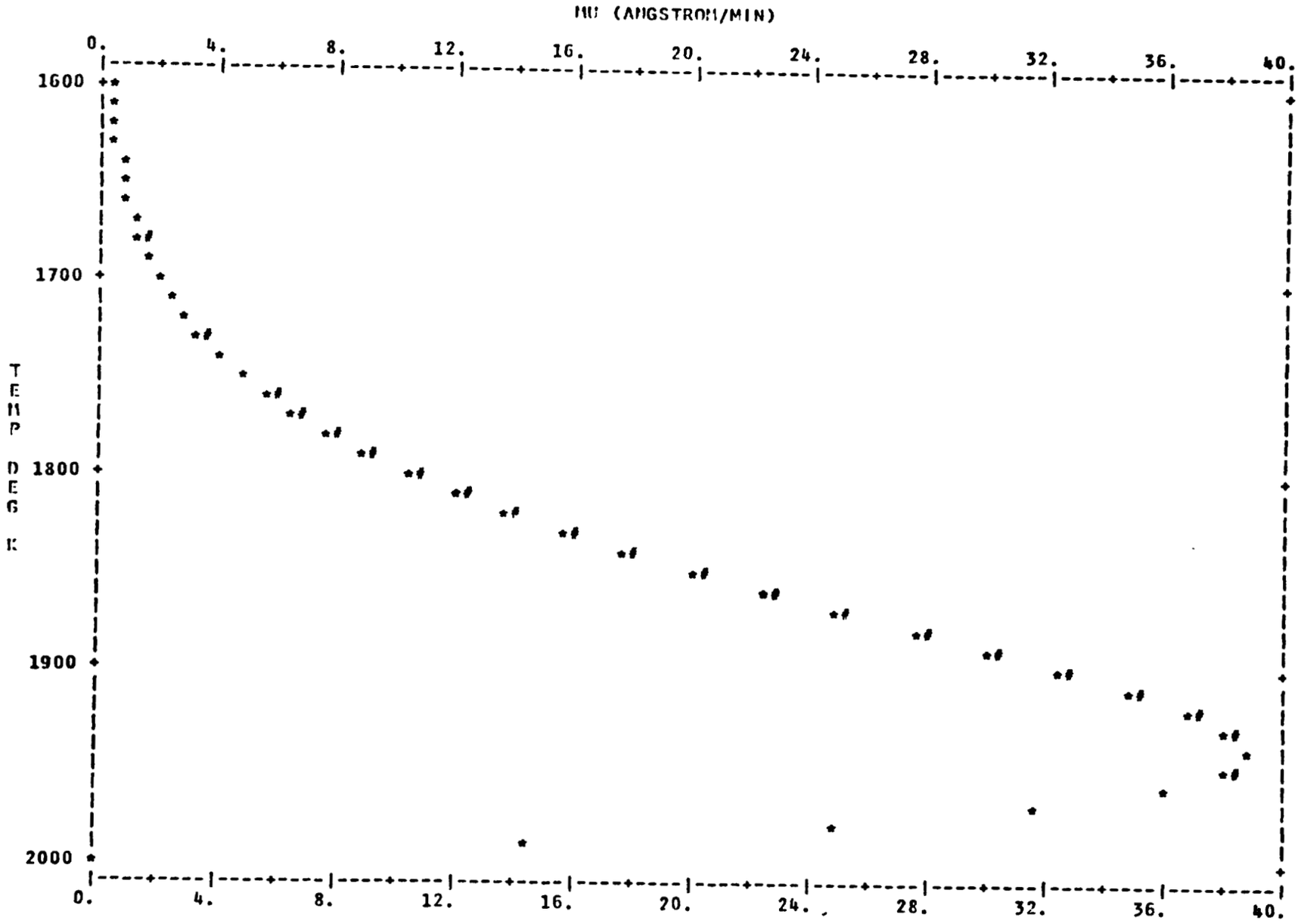

Figure 8 CRYSTAL GROWTH RATE (SiO_2)

below T_m), the free energy term is dominant and increases with increasing supercooling (i.e., the growth rate increases with decreasing temperature). At large degrees of supercooling below T_m, the kinetic factor (diffusion) begins to control, and the growth rate begins to decrease with decreasing temperature. At temperatures far below T_m the diffusion kinetics dominate: the extremely high viscosity inhibits crystal growth, and the growth rate drops to zero.

The critical temperature region for glass forming tendency, the region of simultaneous nucleation and growth, is illustrated qualitatively in Figure 9 in a "T_2-T_3" region plot. If homogeneous nucleation only is considered, it is observed that SiO_2 glass formation depends on the ability to pass through the temperature range $\backsim$ 1600-1700°K rapidly. The transient behavior shown in Figure 7 indicates that this critical region must be traversed in a time less than approximately 5×10^3 sec to avoid the liquid-crystal phase transformation. This time scale limit is readily attained by commercial earth processing methods.

5.2 Hypothetical Glass-Parametric Study

The computer software that has been developed to generate nucleation and growth behavior provides a convenient means of determining which materials parameters are of primary importance in determining glass forming tendency. This information is critical to our overall task of investigating the glass forming tendency of unique systems, or in synthesizing systems for space manufacture.

For this purpose a hypothetical glass was postulated that possessed the viscosity-temperature behavior of SiO_2, and the parameters α and β were varied over realistic ranges (i.e., $2 \leq \alpha \leq 3$, $1 \leq \beta \leq 10$). The resulting parametric graphical representations are presented in Figures 10 and 11, and serve to indicate the importance of these parameters on the (steady state) nucleation rate. The horizontal line is the level of detectability of nucleation (assumed to be 1 nucleus per cm^3 per

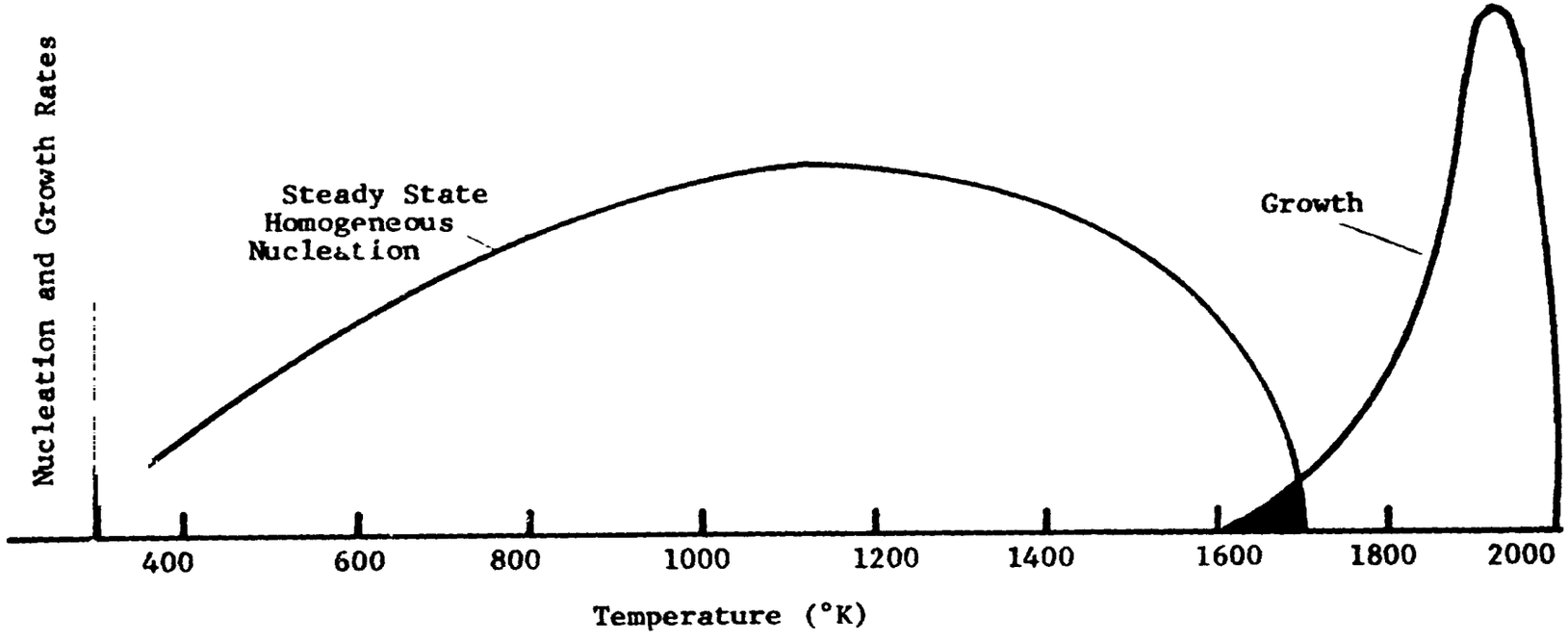

Figure 9 T_2-T_3 REGION NUCLEATION AND GROWTH PLOT FOR SILICA

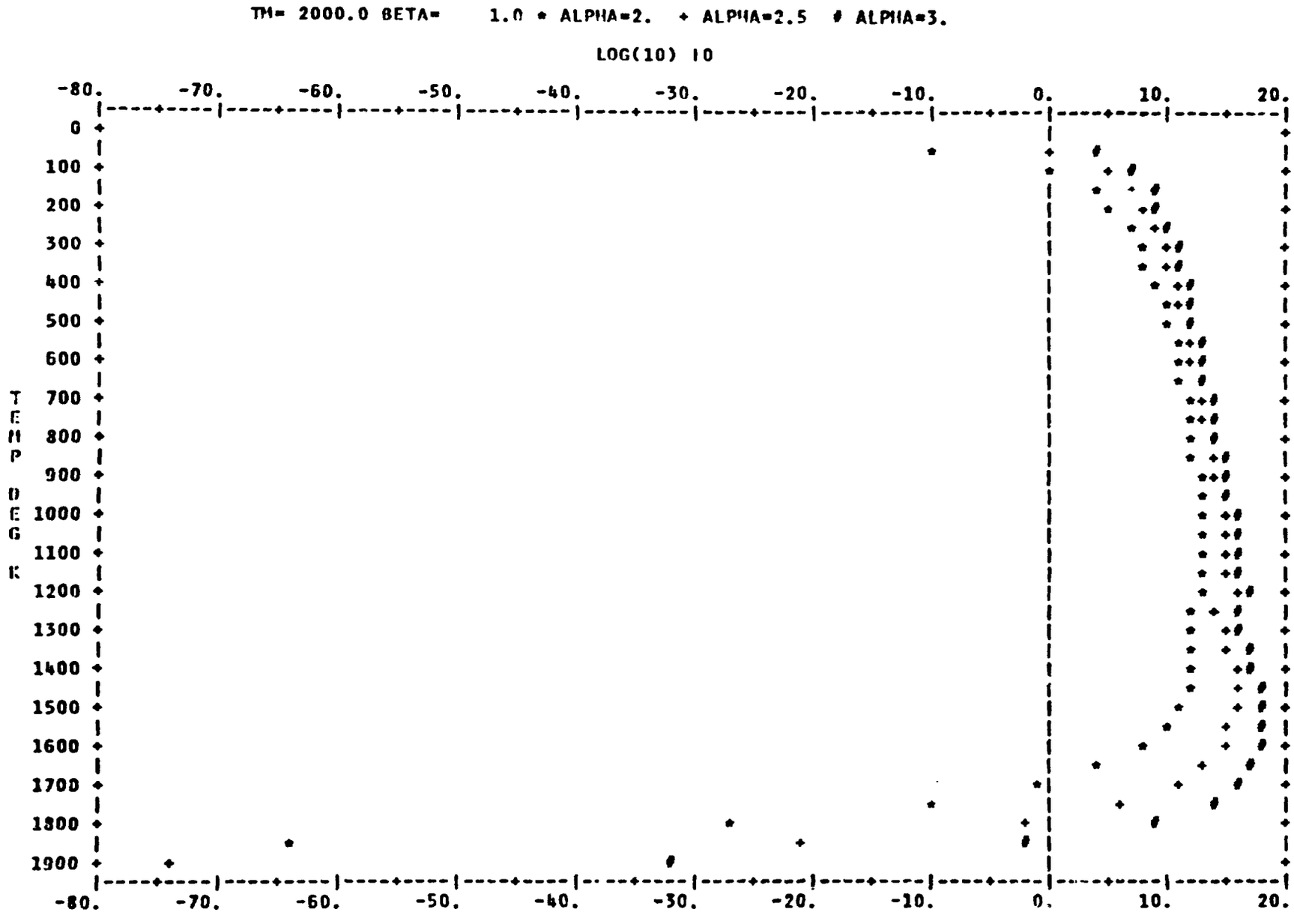

Figure 10 STEADY STATE NUCLEATION RATE FOR A HYPOTHETICAL GLASS (T_m = 2000°K, β = 1, α = VARIABLE); THERMODYNAMIC AND KINETIC BARRIERS

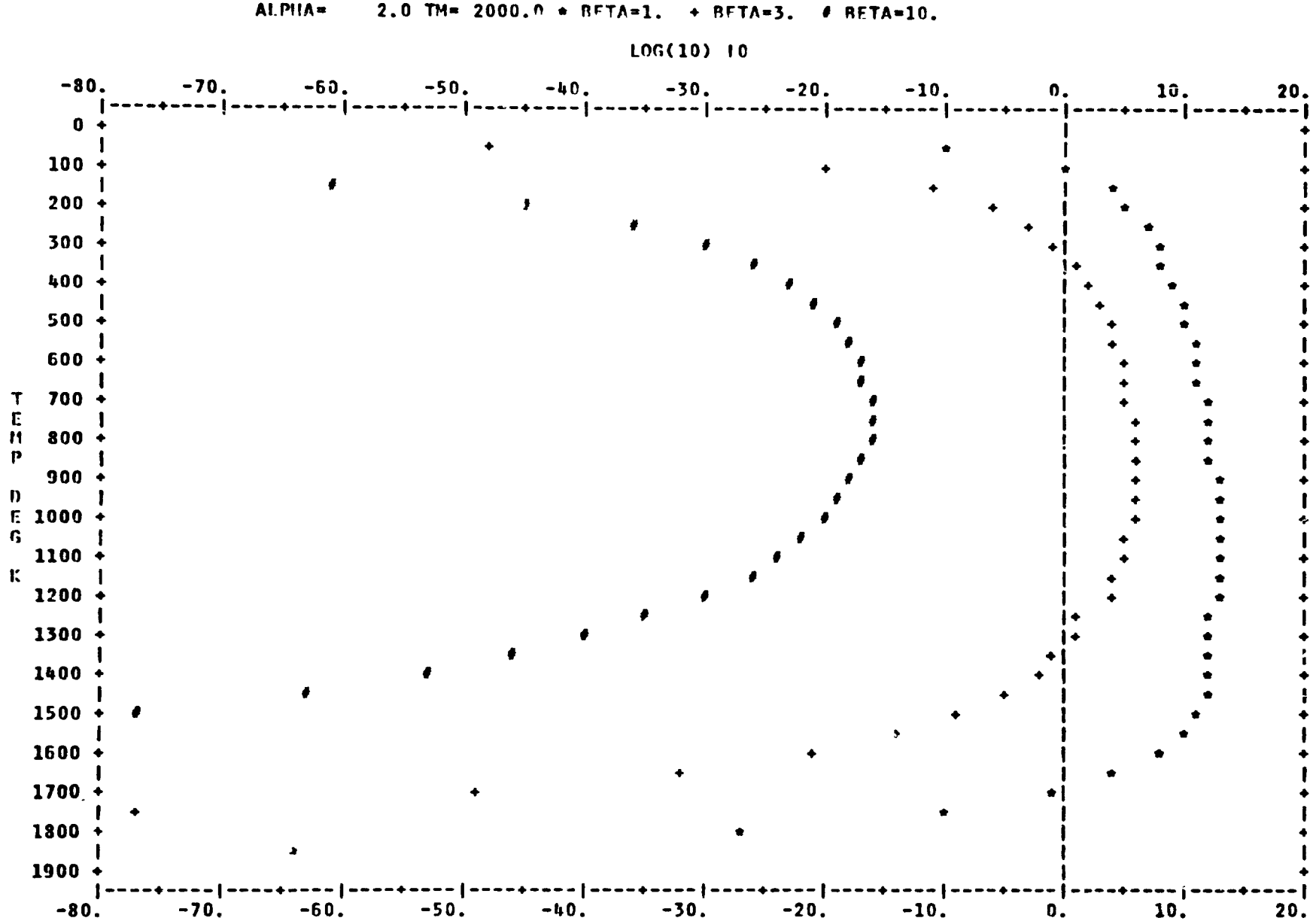

Figure 11 STEADY STATE NUCLEATION RATE FOR A HYPOTHETICAL GLASS (T_m = 2000°K, α = 2, β = VARIABLE); THERMODYNAMIC AND KINETIC BARRIERS

sec). The temperature at which the nucleation curves intersect the horizontal level of detectability line is temperature T_2 shown in Figure 1. Above T_2 no nucleation should be observable. Since nucleation and growth occur simultaneously between T_2 and T_3, we are interested in decreasing (T_2-T_3); therefore, decreasing T_2 will enhance glass forming tendencies. Additionally, we are interested in material parameters that tend to decrease the slope of the nucleation rate-temperature relationship in the region just below temperature T_2 (this is important due to limitations in cooling rates attainable).

Figure 10 illustrates the effect of α for the hypothetical glass with the β parameter fixed at unity. It is observed that decreasing α decreases T_2, and thus tends to increase glass forming tendency.

Figure 11 illustrates the effect of β for the hypothetical glass, with the α parameter fixed at a value of $\alpha = 2$. It is observed that the β parameter has a larger effect on the nucleation rate than does the α parameter. Temperature T_2 decreases with increasing β.

It is apparent that for enhancing glass forming tendencies large β and small α parameters are required. This is based on the observed decrease in the temperature T_2 and decrease in the slope of the nucleation curve near T_2. This can also be seen by considering the expression for ΔF^*, the free energy of a critical embryo, which represents the magnitude of the barrier to nucleation. A large β represents a material with a large heat of fusion; a complicated structure with a large amount of energy involved in the phase change. A small α represents a material with a large heat of fusion relative to the solid-liquid interfacial free energy. Values for β (or Δs_f) for several systems are shown in Table II.

Thus far we have only discussed thermodynamic parameters α and β. Since ther also exists a kinetic barrier to nucleation and growth it would be expected the viscostiy, η, would be a

TABLE II

PERTINENT PROPERTIES OF VARIOUS MATERIALS

Material	Δs_f (cal/mole°K)	Δh_f (cal/mole)	β	T_m(°K)
SiO_2	1	2000	.5	2000
B_2O_3	8.2	5900	4.1	723
GeO_2				
α-Al_2O_3	11.3	26,000	5.6	2300
lithium silicates	5			
potassium silicates	12			
$CaO.Al_2O_3.2\ SiO_2$	16.1			
Soda-Lime glass	8			
Metals	2.3			

parameter of primary importance. Uhlmann (13) has discussed the importance of two kinetic parameters on the tendency of a material to be a glass former: (1) a high viscosity at the fusion temperature, T_m, and (2) a rapidly rising viscosity with decreasing temperature below T_m (i.e., large $d\eta/dT$). The latter is related to the position of T_m relative to the glass transition temperature, T_g. We will not elaborate on the parameters η and $d\eta/dT$ in a parametric study. However, they will be considered in subsequent discussions of the glass forming tendencies of B_2O_3 and Al_2O_3.

5.3 The B_2O_3 System

In this section nucleation and growth kinetics are applied to the B_2O_3 system to predict the observed good glass forming quality for this material, and to imply a physical reason for this phenomena. Qualitative indications of glass forming tendency can be obtained by considering only steady state nucleation, ignoring for the moment transient effects. Steady state data represent an upper bound for nucleation behavior.

The pertinent material properties for the B_2O_3 system are tabulated in Table III. The viscosity of B_2O_3 is illustrated in Figure 12. Over the temperature range 250-500°C the literature data shown were averaged and fit to a 6th degree polynomial expression:

$$\log \eta = AT^6+BT^5+CT^4+DT^3+ET^2+FT+G \qquad (47)$$

with resulting coefficients:

$A = 2.24\times10^{-14}$
$B = -4.56\times10^{-11}$
$C = 3.82\times10^{-8}$
$D = -1.73\times10^{-5}$
$E = 4.81\times10^{-3}$
$F = -8.9\times10^{-1}$
$G = 9.77\times10^{1}$

TABLE III

MATERIALS PARAMETERS FOR B_2O_3

Δh_f = 5900 cal mole^{-1} (reference 21)

T_m = 450°C = 723°K

$\Delta s_f = \frac{\Delta h_f}{T_m}$ = 8.2 cal mole^{-1}K^{-1}

$\beta = \frac{\Delta s_f}{R}$ = 4.1

a_o = 2.5 Å (assumed)

f = 1 (assumed normal growth)

X = 1 (pure substance)

α: variable, $2 \leq \alpha \leq 3$

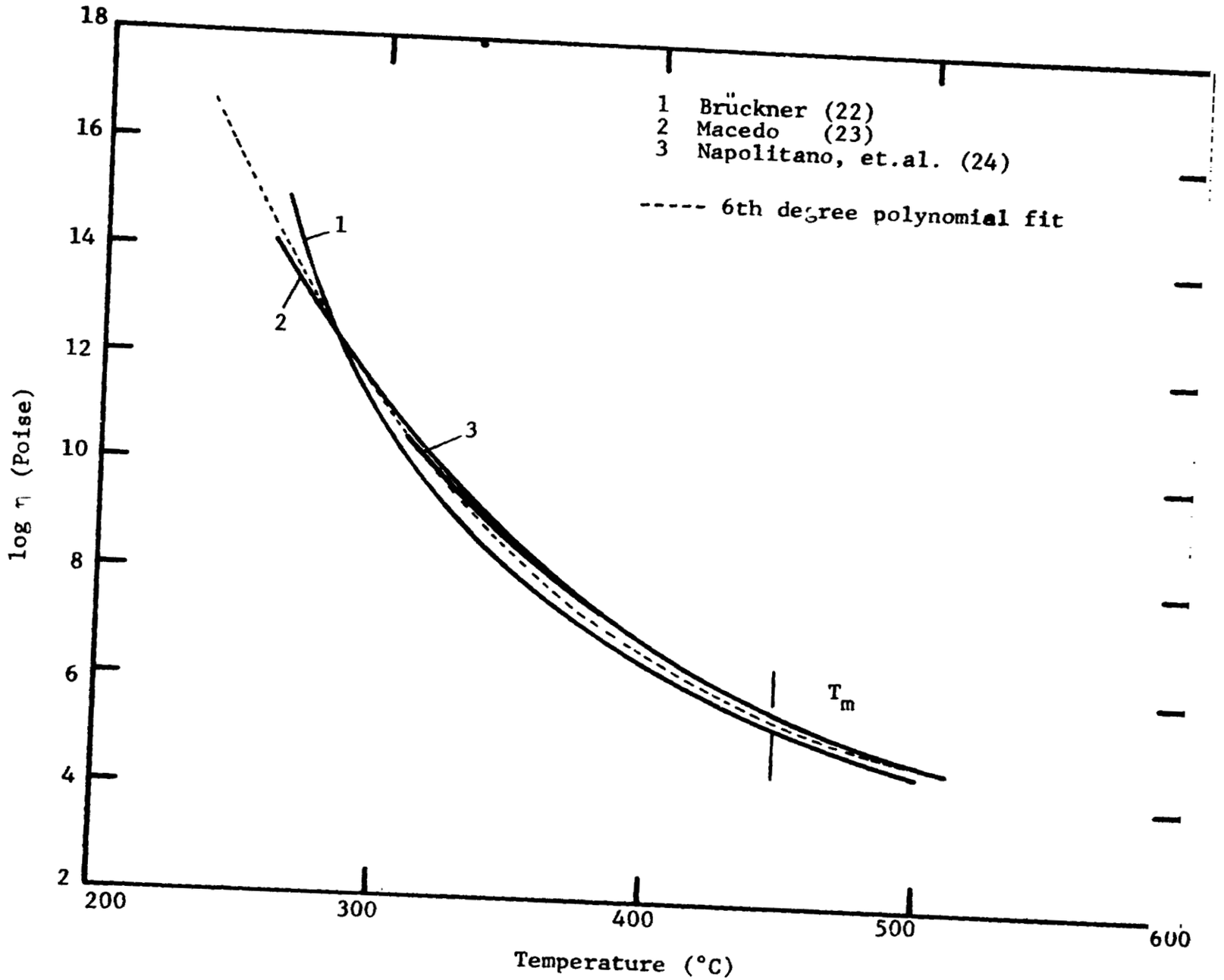

Figure 12 VISCOSITY OF B_2O_3

The computer-generated viscosity data for B_2O_3 are also shown in Figure 12 for comparison.

These material properties were inserted into our computer software and the steady state nucleation rate for B_2O_3 computed and plotted for variable α as illustrated in Figure 13. The computed growth rate for B_2O_3 is illustrated in Figure 14. Glass forming tendency for B_2O_3 is deduced from considerations of the nucleation and growth behavior shown in these two Figures.

Referring to the growth curve (Figure 14), it is observed that the growth rate for B_2O_3 is zero at T_m, peaks at roughly 700°K, and decays to zero by roughly 625°K. The steady state nucleation rate for B_2O_3 (Figure 13) was computed for the known β parameter ($\beta = 4.1$) and for a probable range of the α parameter. It is observed that for all values of α, the nucleation rate is always below the detectable limit (assumed 1 nucleus per cc per sec), and thus effectively zero. Therefore, although B_2O_3 exhibits a theoretical growth rate much higher than SiO_2 (see Figure 8), critical size crystal embryo are never homogeneously nucleated. These analytical results predict, therefore, the B_2O_3 would be an excellent glass former since it can not be made to nucleate and crystallize when cooling from the melt, regardless of the cooling rate. This prediction is supported by empirical evidence indicating that crystallization of B_2O_3 from a dry melt has never been observed. (12)

The parameters of primary importance in describing glass forming tendency from a kinetic standpoint are 1) the magnitude of the viscosity at T_m, 2) the slope of the viscosity-temperature function below T_m, $d\eta/dT$, and 3) the magnitude of the molecular entropy of fusion Δs_f (related to ΔH_f and β). The former two are related to the diffusional barrier and the latter to the thermodynamic barrier to the phase change process, liquid state to crystalline state. The magnitude of the melting point viscosity for B_2O_3 is two orders of magnitude less than that of SiO_2 (see Figure 6). This would indicate that nucleation-crystallization should occur more readily for B_2O_3 (lower diffusional, kinetic

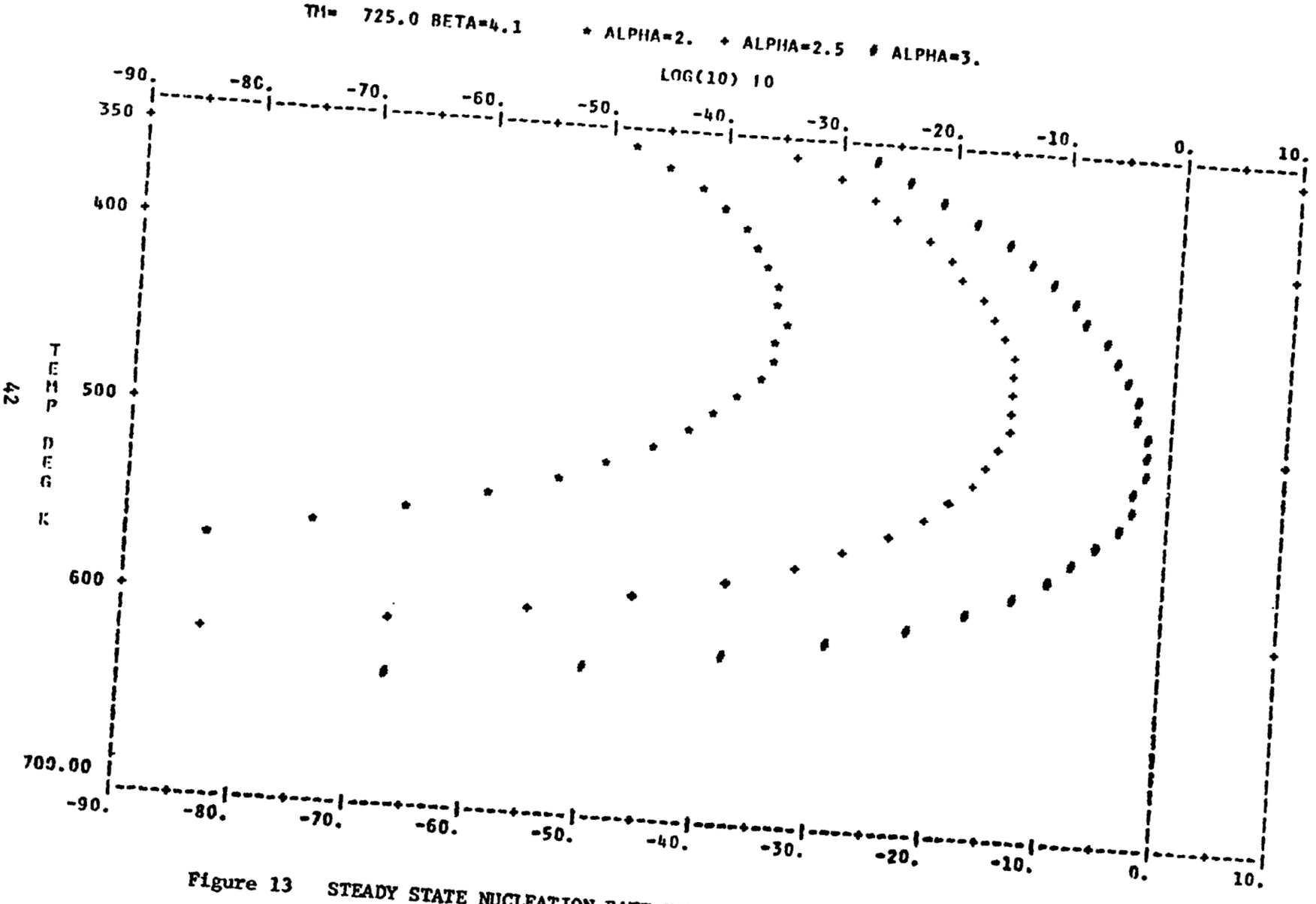

Figure 13 STEADY STATE NUCLEATION RATE FOR B_2O_3 FOR VARIOUS VALUES OF THE α PARAMETER

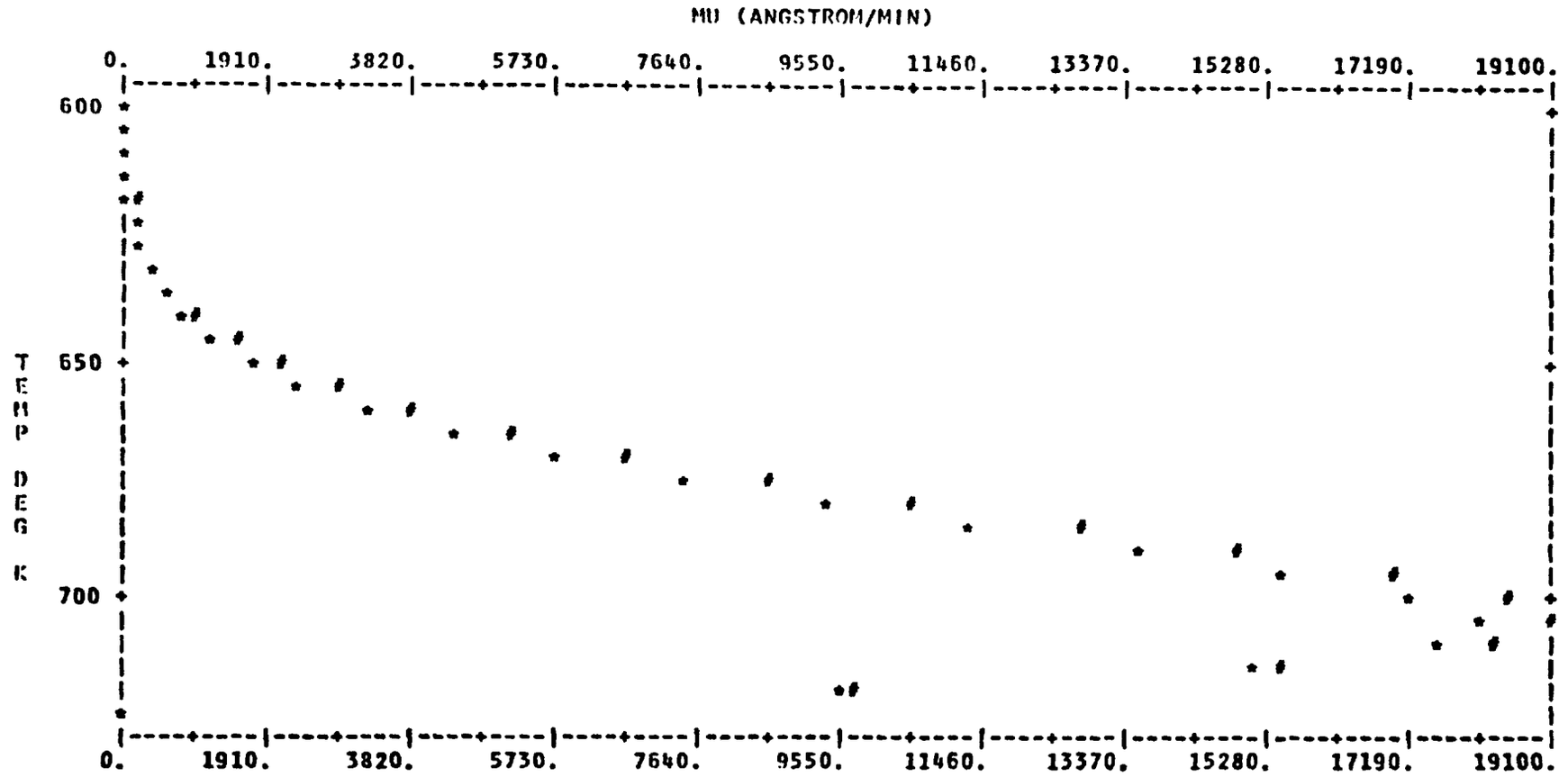

Figure 14 CRYSTAL GROWTH RATE FOR B_2O_3

barrier). Since this is not the case, the factors inhibiting the phase change in B_2O_3 are the high molecular entropy of fusion (8.2 for B_2O_3, roughly 1.0 for SiO_2), and the steepness of the viscosity-temperature relation below T_m for B_2O_3 ($d\eta/dT$ greater for B_2O_3 than for SiO_2 as shown in Figure 6).

To illustrate the relative importance of Δs_f and $d\eta/dT$ in inhibiting nucleation and crystallization in the B_2O_3 system, we have used our computer system to describe the nucleation behavior of a hypothetical liquid with the viscosity-temperature relation of B_2O_3, but with the molecular entropy of SiO_2 (i.e., $\Delta s_f = 1$). Our hypothetical glass then exhibits the kinetics of a material that will not nucleate and crystallize (B_2O_3) and the thermodynamics of a material that will nucleate and crystallize (SiO_2). The nucleation behavior of this hypothetical material is shown in Figure 15, with the behavior of B_2O_3 ($\Delta s_f = 8.2$) also shown for reference. It is observed that the nucleation rate of the hypothetical liquid is now above the detectable limit. Thus by lowering the thermodynamic barrier to the phase change for B_2O_3 (i.e., Δs_f or ϕ) we are able to produce a hypothetical glass that will nucleate. The growth rate for this hypothetical liquid was computed and is shown in Figure 16. Comparing the relative positions of the nucleation and growth curves for this hypothetical liquid (Figures 15 and 16) indicates its glass forming qualities. For convenience these nucleation and growth curves are qualitatively sketched in a "T_2-T_3 region" plot in Figure 17. It is observed that a small region of simultaneous nucleation and growth exists between 625 and 650°K. Thus crystallized B_2O_3 could be obtained upon cooling from the melt (by holding the liquid between 625 and 650°K) if the molecular entropy of fusion (or heat of fusion) could be reduced substantially. This hypothetical example is presented as an indication of how we might eventually be able to synthesize materials to exhibit desired nucleation-crystallization tendencies.

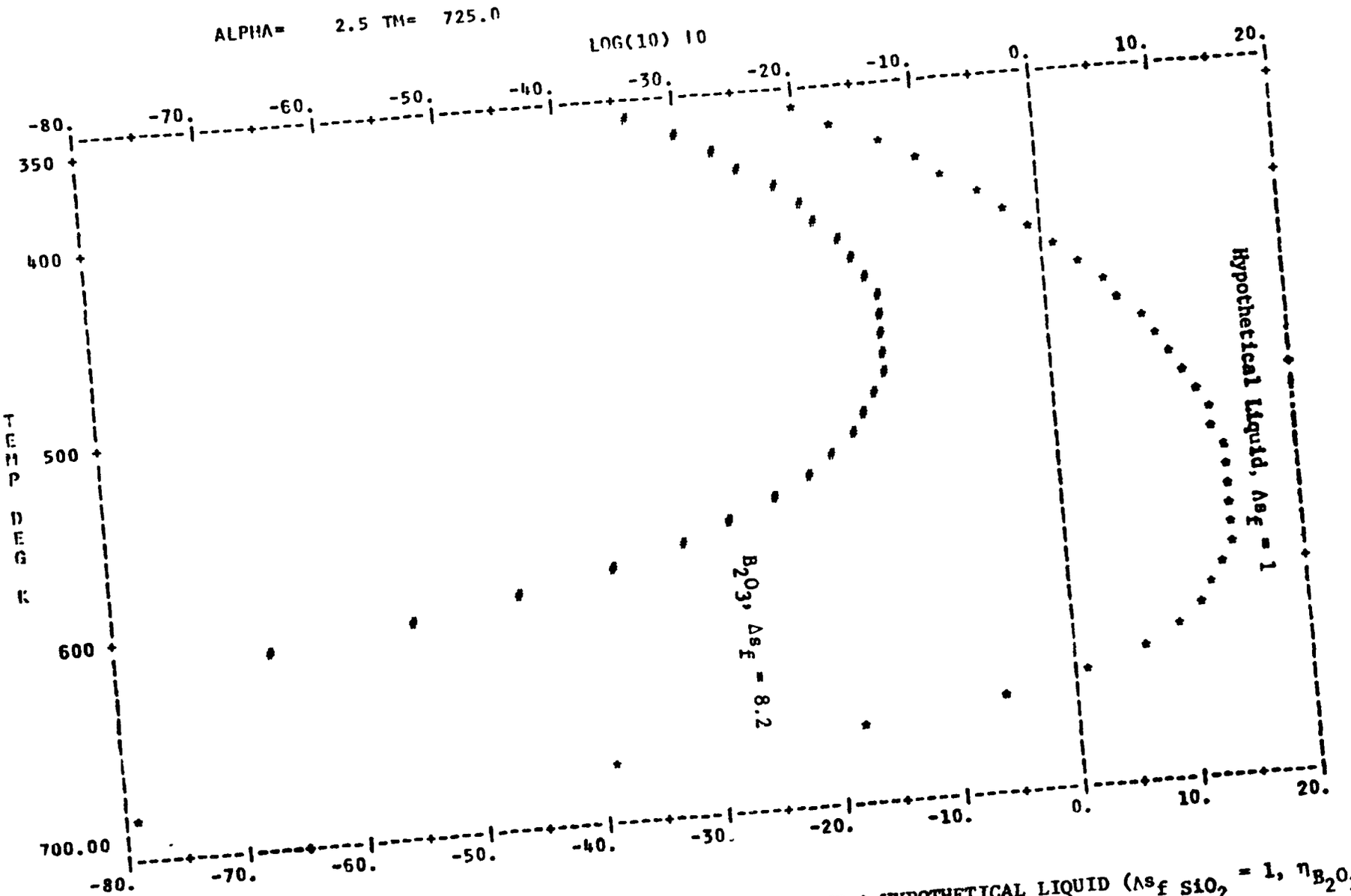

Figure 15 STEADY STATE NUCLEATION RATE FOR B_2O_3 AND A HYPOTHETICAL LIQUID (Δs_f SiO_2 = 1, $\eta_{B_2O_3}$)

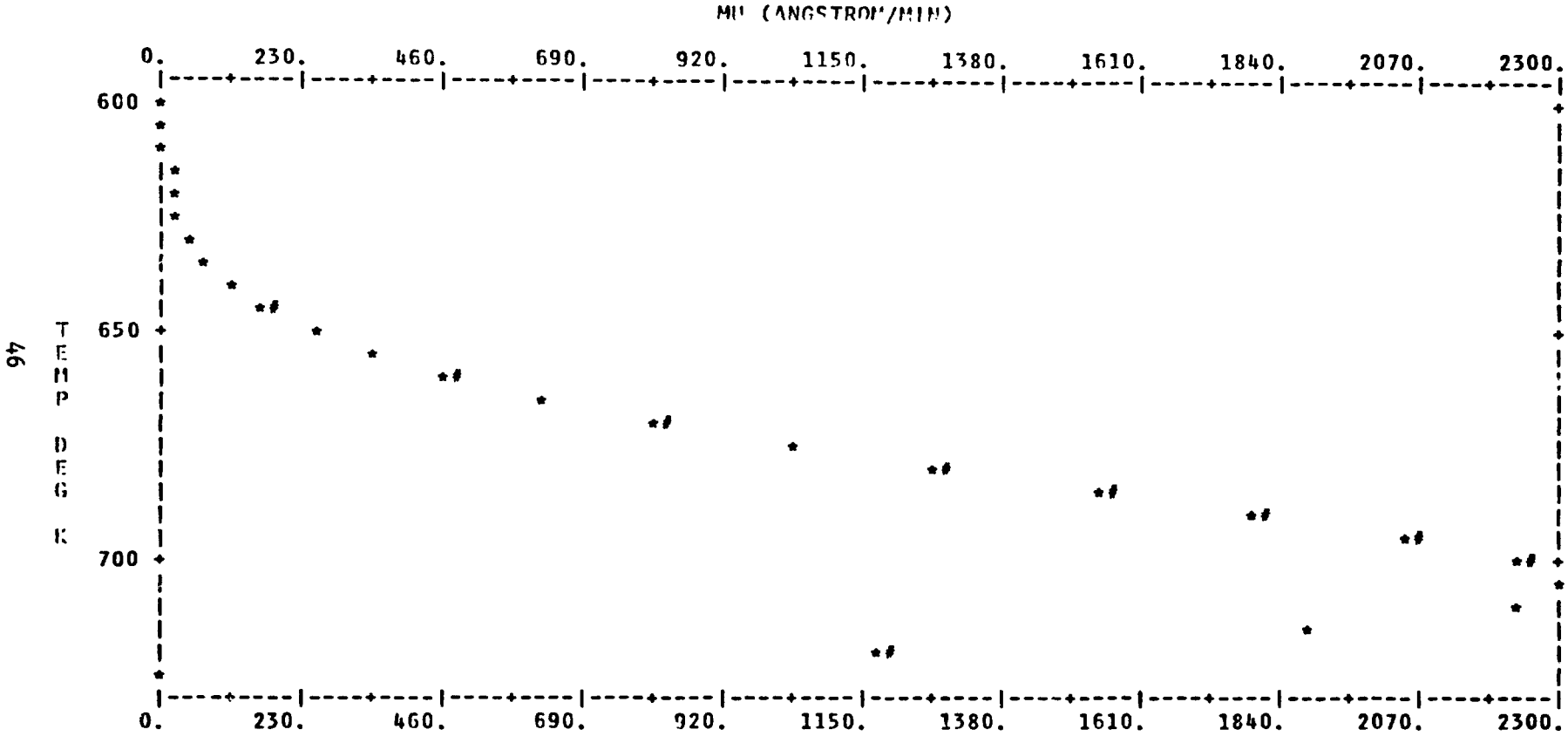

Figure 16 CRYSTAL GROWTH RATE FOR A HYPOTHETICAL LIQUID ($\Delta s_{f\ SiO_2} = 1$, $\eta_{B_2O_3}$)

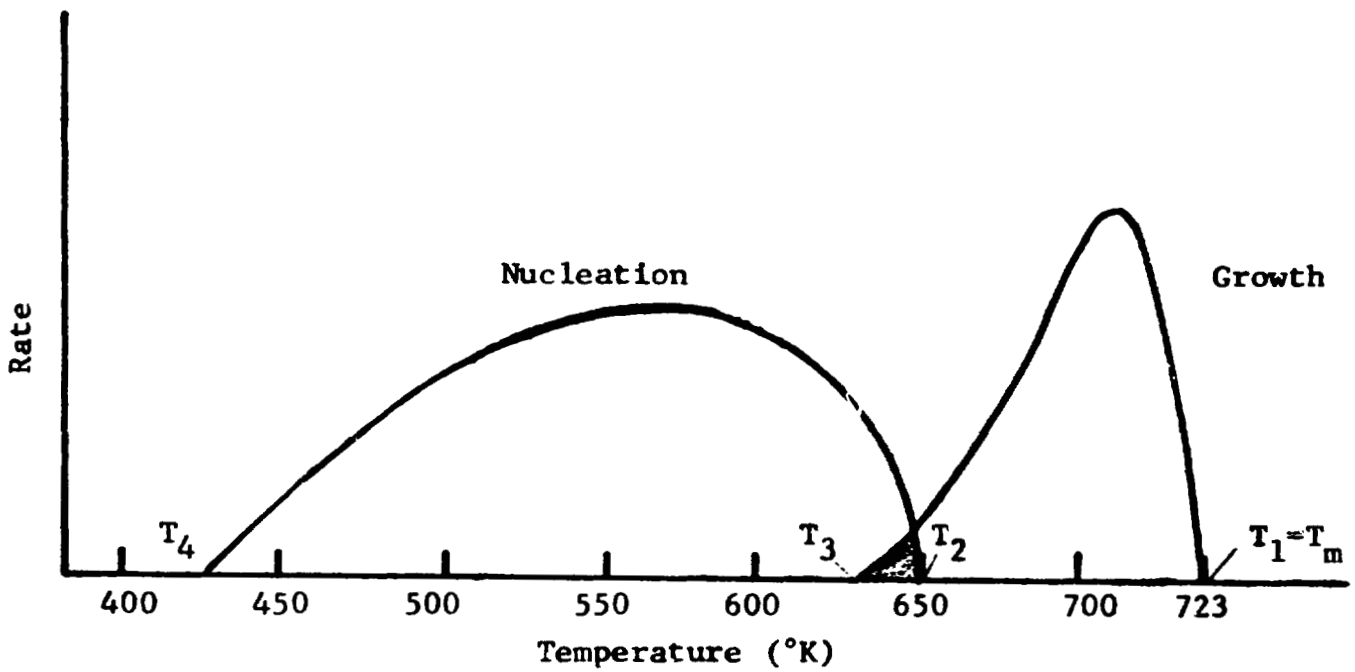

Figure 17 NUCLEATION AND GROWTH CHARACTERISTICS OF A HYPOTHETICAL LIQUID ($\eta_{B_2O_3}$, β_{SiO_2}, $\alpha = 2.5$)

5.4 The Al_2O_3 System

Nucleation and growth kinetics also have been applied to the Al_2O_3 system. This system exhibits very poor (non-existent) glass forming tendencies by conventional earth methods. The aim here is to predict this poor glass forming tendency of Al_2O_3 and imply a physical reason for this phenomenon.

The pertinent materials properties for the alumina system are tabulated in Table IV. The major difficulty in describing nucleation and growth kinetics for the Al_2O_3 system is the complete lack of viscosity data below the fusion temperature, T_m. This situation exists since Al_2O_3 has never been observed on earth as a glass (i.e., at temperatures below T_m). Above the melting point, however, data have been reported,[17] and are illustrated in Figure 6. With no reference point such as the glass transition, T_g, available, the problem remains as to the shape of the viscosity-temperature curve for Al_2O_3 below T_m. For our purposes we have chosen two cases: 1) extrapolating below T_m with the shape of the B_2O_3 curve (i.e., steep $d\eta/dT$) and 2) extrapolating below T_m with the shape of the SiO_2 curve. These two cases thus represent the upper and lower bounds for $d\eta/dT$ of the various oxides shown in Figure 6. For both cases the extrapolated curves were expressed algebraically using curve fitting techniques for use in our computer software.

The homogeneous nucleation and growth characteristics of Al_2O_3 are summarized in the "T_2-T_3 region" plot shown in Figure 18. Behavior depicted by solid lines represents the case where Al_2O_3 is assumed to have a $d\eta/dT$ behavior below T_m similar to that of SiO_2 (see Figure 6). The dotted lines in Figure 18 represent the case where the viscosity-temperature dependence of B_2O_3 is assumed below the Al_2O_3 fusion temperature, T_m. Since Al_2O_3 has such a low viscosity at its fusion temperature (melting point), theoretical growth rates are much higher than for either pure SiO_2 or B_2O_3. Both of the Al_2O_3 growth

TABLE IV

MATERIALS PARAMETERS FOR Al_2O_3

T_m = 2300°K

a_o = 2.5 Å (assumed)

f = 1 (assumed)

Δh_f = 26,000 cal $mole^{-1}$ (reference 21)

$\Delta s_f = \frac{\Delta h_f}{T_m}$ = 11.3 cal $mole^{-1}K^{-1}$

$\beta = \frac{\Delta s_f}{R}$ = 5.65

α = 2, 2.5, 3 (variable)

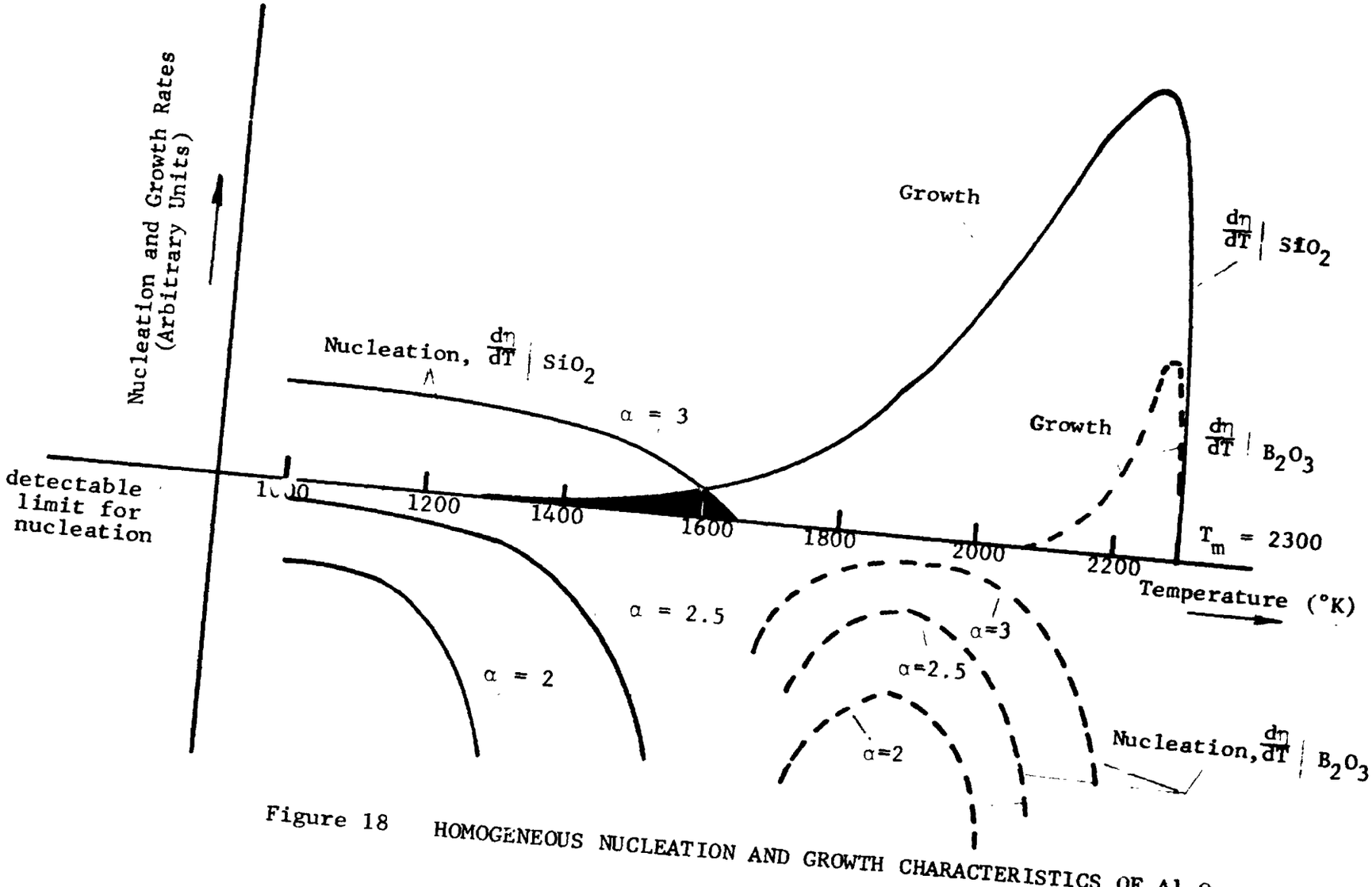

Figure 18 HOMOGENEOUS NUCLEATION AND GROWTH CHARACTERISTICS OF Al_2O_3

rate curves shown in Figure 18 have peak magnitudes of $\backsim 10^{10}$ Å/min, compared to 40 Å/min for SiO_2 (Figure 8) and 2×10^4 Å/min for B_2O_3 (Figure 14). To illustrate the very large theoretical growth rate of Al_2O_3, the peak growth of B_2O_3 (2×10^4 Å/min) is reached by the alumina system within $\backsim 10^{-5}$°K undercooling below T_m. The 40 Å/min peak growth rate of SiO_2 is reached by Al_2O_3 within $\backsim 10^{-8}$°K undercooling below T_m.

At large degrees of undercooling below T_m, in the diffusion-controlled portion of the growth curve, the steepness of the viscosity-temperature relation is seen to determine the temperature at which the growth rate drops to zero. Since we are dealing with the approximate upper and lower boundaries of the possible viscosity relation of alumina below T_m, this temperature (T_3 in a conventional "T_2-T_3 region" nucleation and growth plot) lies between approximately 1300° and 2050°K.

The steady state homogeneous nucleation rate for Al_2O_3 is also shown in Figure 18 (for α variable). For the condition where the Al_2O_3 viscosity has the general temperature dependence of B_2O_3 below T_m (steep $d\eta/dT$) it is observed that homogeneous nucleation is below the detectable limit. Where Al_2O_3 is assumed to behave more like SiO_2, which is more probable, it is observed that a detectable level of homogeneous nucleation occurs for $\alpha=3$. The shaded region shown in Figure 18 thus represents the region of simultaneous (homogeneous) nucleation and crystal growth for Al_2O_3 system.

If homogeneous nucleation and subsequent growth are considered, we have shown that to avoid crystallization upon cooling from the melt the temperature region 1300° to 1625°K must be passed through rapidly. In practice, however, Al_2O_3 is known to crystallize almost immediately upon cooling below the fusion temperature, T_m (2300°K). The reason for this discrepancy is that our analytical predictions of glass forming tendency have not accounted for heterogeneous nucleation. In the case of heterogeneous nucleation any insoluble inpurity or

external surface will serve to lower the size of a critical embryo and thus effectively increase temperature T_2 (the temperature where detectable nucleation first appears upon cooling from the melt). This effect is shown in Figure 19. Temperature T_2, corresponding to homogeneous nucleation, is shifted to a higher temperature (T_2') if heterogeneous nucleation is possible (i.e., if extrinsic nucleation sites are present). As illustrated in Figure 19, simultaneous heterogeneous nucleation and growth can (qualitatively) occur at temperatures just below the fusion temperature, T_m. Most investigators of crystallization phenomena indicate that nucleation appears to initiate heterogeneously in most materials. Thus an extrinsic property controls the glass forming tendency of Al_2O_3, at least on earth where the complete elimination of heterogeneous nucleation sites is not possible. Complete elimination of external nucleation sites in Al_2O_3 is necessary if Al_2O_3 glass is to be obtained since the growth rates are so high. Therefore, Al_2O_3 might be a good candidate for space manufacture since processing could be performed containerless, with no external surfaces acting as nucleation sites. Before the space-processing candidacy of Al_2O_3 is determined, however, several areas must be investigated in more detail. These include: 1) glass quality regarding crystal size and concentration if homogeneous nucleation only is possible (i.e., considering the high growth rates and attainable quench rates from 1625° to 1300°K, perhaps enough crystalline phase would be nucleated homogeneously to yield a poor quality glass even with space processing), and 2) insoluble impurity levels attainable in Al_2O_3 precursor materials (i.e., perhaps enough impurity sites will be available for heterogeneous nucleation to make elimination of surface nucleation sites (crucible wall) through space processing only a second order improvement). Clearly, if space processing is to be employed to eliminate heterogeneous nucleation sites leading to high quality glasses, then the mechanisms of heterogeneous nucleation must be well known before candidate materials can be chosen with any confidence.

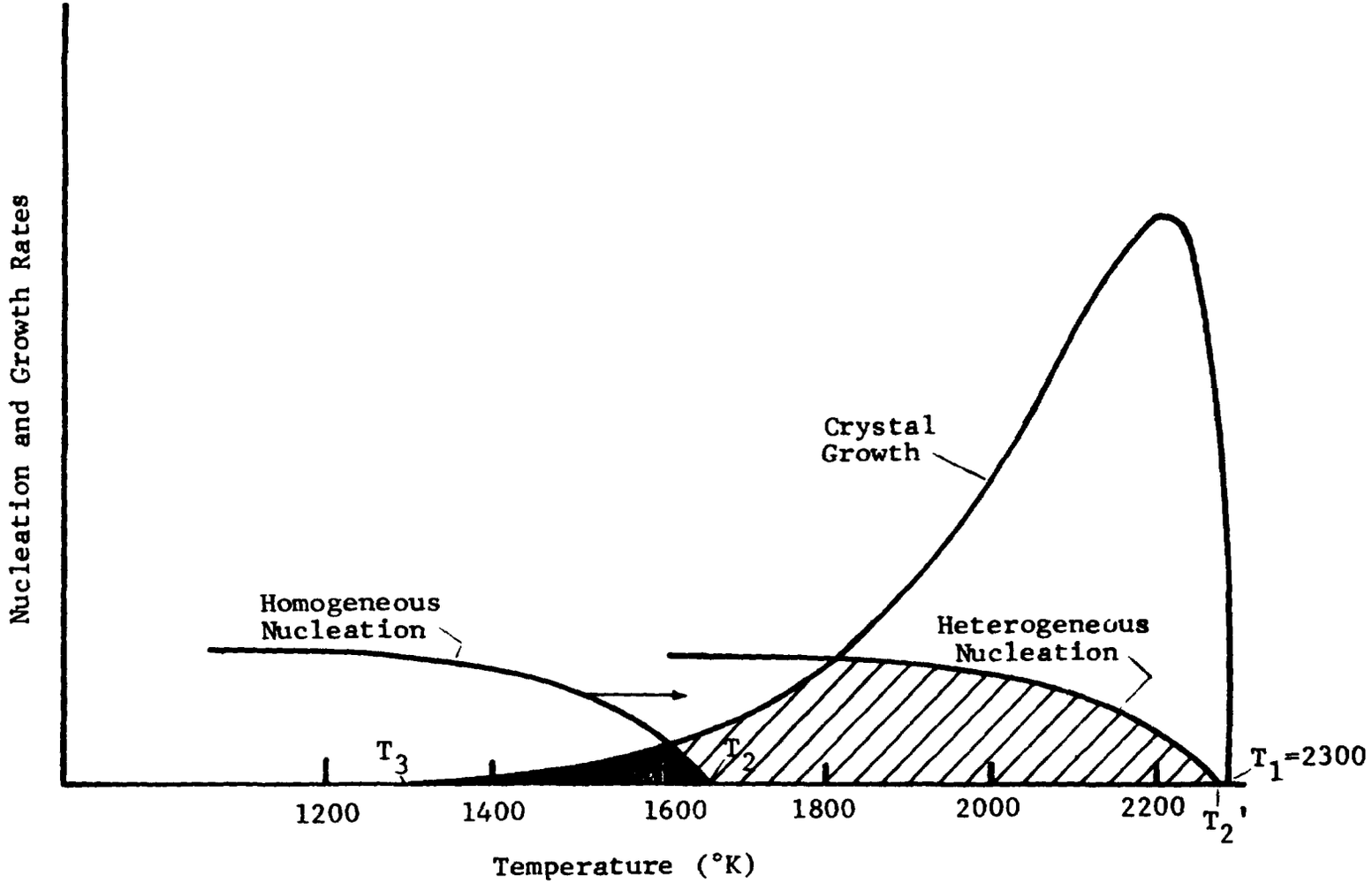

Figure 19 EFFECT OF HETEROGENEOUS NUCLEATION ON GLASS FORMING TENDENCY OF Al_2O_3

6.0 APPLICATIONS TO MORE COMPLEX SYSTEMS

The nucleation and growth kinetics that have been developed in Section 3 apply in general to single component substances or congruently melting (i.e., without composition change) compounds. The liquid-solid transformation process for these materials is termed non-reconstructive. No interatomic bonds within the participating molecules need be broken, and only short range diffusion processes are required for the transformation to occur at the liquid-crystal interface. In this instance, the molecular movements are treated as simply activated processes, with rate constants approximately equal to the coefficient of self-diffusion in the bulk liquid. This is convenient since the self-diffusion coefficient is related to the viscosity through the Stokes-Einstein equation, and viscosity data are more readily attainable kinetic data than diffusion data.

In multicomponent systems, however, the liquid to solid transformation often involves bond breaking and/or long-range diffusion processes, as discussed previously. In this instance the transformation is termed reconstructive. In network liquids, such as SiO_2, interatomic bonds must be broken in the network prior to molecular rearrangement. Since this bond breaking in network liquids must also preceed viscous flow or self-diffusion, the free energy of activation for these processes will also be applicable as the kinetic barrier to the phase charge process (25). Thus, in the reconstructive transformation of a network liquid we can approximate the activation energy and the rate constant in the same manner as for non-reconstructive crystallization:

$$\Delta G'(\text{nucleation}) = \Delta G''(\text{growth}) = \Delta G_a \text{ (flow activation energy)} \quad (48)$$

and,

$$D_n \cong D_g \cong D_s = \frac{kT}{3\pi a_o \eta} \quad (49)$$

However, in reconstructive crystallization where a large change in composition is involved, long range diffusion processes are required to bring the appropriate atomic species to the liquid-

crystal interface. In this case the rate limiting step may be the diffusion of a particular (i.e., the slowest moving) species in the liquid matrix. In dealing with nucleation and growth kinetics and subsequent glass forming tendency of such materials, several methods have been postulated. Uhlmann and Chalmers (8) suggest that for nucleation involving large changes in composition that the kinetic barrier to nucleation, $\Delta G'$ in Equation (20), should be taken as the activation energy for diffusion of the slowest moving component in the matrix, and that the pre-exponential factor, $n\nu$, should be reduced by the mole fraction of the precipitating component. This presents a problem since the appropriate diffusion data are not as readily available as bulk liquid viscosity data. Furthermore, the kinetic term for nucleation, $\Delta G'$, is not necessarily equal to or even the same order of magnitude as the kinetic term for growth, $\Delta G''$ in Equation (32). This is due to the fact growth is governed by atomic movements from a great distance from the interface, whereas the molecular movement involved in the nucleation process occurs relatively near the liquid-crystal interface. In general, growth in multicomponent systems where composition is a variable tends to be diffusion-controlled rather than interface-controlled. Hammel (4) has discussed the formulation for computing the volume fraction of material transformed for diffusion controlled growth:

$$v_f = \frac{8\pi}{15} S^3 D'^{3/2} I_o t^{5/2} \qquad (50)$$

where D' is the diffusion rate constant and S is a supersaturation term. Again, however, diffusion coefficients are required that are not readily available.

The question arises, then, of how we can predict the glass forming tendency in systems where diffusion controlled behavior is expected due to large compositional changes during the transformation, and for which the required diffusion data are not available. Hillig (11,26) has proposed that incorporation of a transient nucleation rate (5) will adequately account

for long range diffusional effects that occur in a reconstructive transformation. Hammel (4) has applied transient nucleation analysis (Equations 26, 27, 28) and diffusion controlled growth analysis (Equation 50) to predict the volume fraction of cristobalite (SiO_2) precipitating from E glass ($13NaO_2 \cdot 11CaO \cdot 76SiO_2$) during cooling from the melt. In the nucleation rate expression Hammel used a value of X = .1 (mole fraction of precipitating phase in the melt, Equation 28) to account for the long range molecular rearrangement. A value of X equal to unity is employed for a pure single component substance or a congruently melting compound. The determination of the appropriate value for X to use in a given reconstructive transformation is not clearly defined, however. Hammel (27) and Hillig (26) have proposed that X be determined by considerations of 1) what the expected rate-limiting species will be and 2) its concentration in the melt. In Hammel's treatment of diffusion controlled growth described above, a value of S in Equation (50) was determined using Frank's (28) tabulated values for diffusion controlled growth.

Unfortunately, the state-of-the-art in this nucleation-crystallization area has not reached the point where predicted transformation kinetics correlate well with reality in all instances. Especially in the case where large composition changes accompany the transformation, we may have to resort to empirically derived nucleation and growth kinetics as discussed by Uhlmann (12).

7.0 CONCLUSION AND FUTURE WORK

The emphasis in this program is in developing the analytical tools to permit prediction of glass forming tendency in unique oxide systems. Unique systems, for our purposes, means systems that are not good glass formers by conventional Earth-processing means.

A fairly comprehensive treatment of nucleation and growth kinetics in pure substances has been presented. The derived transformation kinetics have been successfully applied to a well-characterized system (SiO_2), an excellent glass former (B_2O_3), and a poor glass former by conventional means (Al_2O_3). The kinetic and thermodynamic parameters of viscosity and entropy of fusion have been shown to be the primary materials parameters controlling glass forming tendency.

For complex multicomponent systems where diffusional effects predominate, the state-of-the-art is not nearly as far advanced as for simple substances. The transformation kinetics of materials which crystallize with a large compositional change are most probably governed by the long range diffusion of the slowest moving species. The general lack of specific diffusion data, however, dictate that simplifying assumptions be made, such as the validity of the Stokes-Einstein equation relating bulk diffusion and viscosity.

With the nucleation and growth kinetics that have been developed, we can now begin to determine how a processing technique such as space processing can be utilized to produce technically significant glasses unobtainable on Earth. Our work has lead us to the point where we need to achieve a better understanding of real, nonsimple systems. This mainly involves a better understanding of diffusion-controlled kinetics and effects of heterogeneous nucleation phenomena. Since adequate literature data to be used in our analytical relationships are non-existent we must rely on empiricism. A series of actual melt-quench

experiments in the laboratory will permit us to correlate the behavior of potential space processing candidates with the theory and analytics that have been developed. It is believed that the coupling of our kinetic equations with empirical evidence and post-quench examination will permit reasonably accurate predictions of the glass forming tendency in unique systems. Our goal is to be able to predict the level of product improvement that is obtainable through in-space materials processing.

To achieve this objective we shall employ our idealized kinetics to try to extend the glass forming region of calcium aluminate, Y_2O_3, Ga_2O_3, and mullite, for instance. The subject of glassy mullite compositions is currently receiving attention in the literature, and calcium aluminate has application (for high alumina concentrations) in ir-transmitting systems (i.e., sapphire is a well known ir-transmitting material).

To facilitate the correlation of theory and experiment we are currently working with the North American Rockwell group* whose program entails the production of unique glasses by a laser spin melting technique. In this cooperative effort we shall conduct a series of experiments designed to aid in the determination of candidate space processing materials, and to predict the level of product improvement to be expected in space manufacture. Specifically, the experimental observations will help us to fit heterogeneous nucleation and diffusion controlled behavior into our kinetic equations in the absence of the required literature data (such as surface energies, wettability, and diffusion coefficients). Areas of investigation in this cooperative effort include 1) degree of superheat (above T_m) necessary to eliminate volume heterogeneous nucleation (impurity) sites, 2) effectiveness of containerless processing in eliminating surface heterogeneous nucleation sites, 3) cleanliness of the sample environment (atmosphere) required in space processing of unique materials, etc.

---

* NASA Contract NAS8-28991, R. A. Happe, Principle Investigator.

The results of this work will appear in subsequent progress reports.

Respectfully submitted,
IIT RESEARCH INSTITUTE

D. C. Larsen
Associate Research Engineer
Ceramics Research Section

APPROVED:

S. A. Bortz
Assistant Director
Mechanics of Materials
Research Division

References

1. Morey, G.W., The Properties of Glass, Reinhold, New York, 2nd Edition (1959).

2. Jackson, K.A. "Nucleation From the Melt", Nucleation Phenomena, American Chemical Society, 1966.

3. Turnbull, D. "Thermodynamics and Kinetics of Formation of the Glass State and Initial Devitrification", Physics of Non-Crystalline Solids, Proc. Int'l. Conf., Delft (1964), J.A. Prins. ed.

4. Hammel, J.J., "Nucleation in Glass Forming Materials", Chapter in Nucleation, A.C. Zettlemoyer, ed., Marcel Dekker, N.Y. (1969).

5. Hillig, W.B., "A Theoretical and Experimental Investigation of Nucleation Leading to Uniform Crystallization of Glass", Symposium on Nucleation and Crystallization in Glasses and Melts, American Ceramic Society, 1962.

6. Collins, F.C., Z. Elektrochem. 59 404 (1955).

7. Turnbull, D. and Cohen, M.H., "Crystallization Kinetics and Glass Formation", Modern Aspects of the Vitreous State, Vol. 1. J.D. Mackenzie, ed., Butterworths, London (1960).

8. Uhlmann, D.R. and Chalmers, B., "The Energetics of Nucleation" Nucleation Phenomena, Am. Chem. Soc. (1966).

9. Hammel, J.J., "Nucleation in Glass - A Review", Adv. Nucleation and Crystallization in Glasses, Glass Division Symposium, Am. Ceram. Soc., Sp. Publ. #5 (1971), L.L. Hench and S.W. Freiman, eds.

10. Rawson, H., Inorganic Glass-Forming Systems, Academic Press, New York (1967).

11. Hillig, W.B., "Glass as a Medium for Controlling Physiochemical Reactions" in Reactivity of Solids, J.W. Mitchell, et. al. eds., Wiley (1969).

12. Uhlmann, D.R., "Crystal Growth in Glass-Forming Systems - A Review", Adv. Nucleation and Crystallization in Glasses, American Ceramic Society Sp. Publ. #5, L.L. Hench and S.W. Frieman, eds. (1971).

13. Uhlmann, D.R., "A Kinetic Treatment of Glass Formation" J. Non-Cryst. Solids 7,337-48 (1972).

14. Mackenzie, J.D., J. Am. Ceram. Soc. 44 (12), 1961 (from Parks and Spaght, Physics 6 (2) 1935.)

15. IITRI Measured Container Compostion: $71SiO_2 \cdot 15Na_2O \cdot 8CaO \cdot 4.5MgO \cdot 1.5 Al_2O_3$

16. Reibling, E.F., J. Chem. Phys. 39 (7) 1963.

17. "Recommended Values of the Thermophysical Properties of Eight Alloys, Major Constituents and Their Oxides," unpublished compilation of data from Thermophysical Properties Research Center, Purdue University (1966); Source of Data: Kozakevitch, P., Met. Soc. Conf. 7, 97 (1961).

18. Fontana, E.H. and Plummer, W.A., "A Study of Viscosity - Temperature Relationships in the GeO_2 and SiO_2 Systems," Phys. Chem. Glasses 7 (4) 1966.

19. Bacon, J.F., et. al. "Viscosity and Density of Molten Silica and High Silica Content Glasses," Phys. Chem. Glasses 1(3) 1960.

20. Bruckner, R., "Properties and Structure of Vitreous Silica," J. Non-Cryst. Solids 5 (3) 1970.

21. JANAF Thermochemical Data Tables.

22. Bruckner, V.R., Glass Tech. Ber. 37 (H9) 413 (1964).

23. Macedo, P.B., and Napolitano, A., J. Chem. Phys. 49(4) 1887 (1968).

24. Napolitano, A., Macedo, P.B. and Hawkins, E.G., "Viscosity and Density of Boron Trioxide," J. Am. Ceram. Soc. 48(12) 613 (1965)

25. Turnbull, D. and Cohen, M.H., "Concerning Reconstructive Transformation and Formation of Glass," J. Chem. Phys. 29(5), 1958.

26. Hillig, W.B., Private Communication.

27. Hammel, J.J., Private Communication.

28. Frank, F.C., Proc. Roy. Soc. (London) A201, 586 (1950).

BIBLIOGRAPHY

29. Avrami, M., "Kinetics of Phase Change - II: Transformation-Time Relations for Random Distribution of Nuclei." J. Chem. Phys. 8 212 (1940).

30. Berezhnoi, A.I., Glass Ceramics and Photo-Sitalls, Chapter II "The Formation of Nuclei and the Crystallization of Glass," Mercol, S.A., Pincus, A.G. (trans.) Plenum, N.Y. (1970).

31. Binsbergen, F.L. "Computer Simulation of Nucleation and Crystal Growth, "J. Cryst. Growth. 16 249 (1972).

32. Binsbergen, F.L. "Study of Molecular Phenomena in the Nucleation of Crystallization by Computer Simulation and Application to Polymer Crystallization Theory," J. Cryst. Growth 13/14 44 (1972).

33. Buckle, E.R., "Studies on the Freezing of Pure Liquids, II. The Kinetics of Homogeneous Nucleation in Supercooled Liquids," Proc. Roy. Soc. (London) A261 189 (1961).

34. Calvert, P.D. and Uhlmann, D.R., "Surface Nucleation Growth Theory for the Large and Small Crystal Cases and the Significance of Transient Nucleation," J. Cryst. Growth 12 291 (1972).

35. Cooper, A.R., "Crystal Growth in Network Liquids by Structure Rearrangement," in Adv. Nucleation and Crystallization in Glasses, L.L. Hench and S.W. Frieman, eds., Am. Ceram. Soc. Sp. Publ. #5, (1971).

36. Cooper, A.R. and Gupta, P.K., "Analysis of Diffusion Controlled Crystal Growth in Multicomponent Systems," ibid, pg. 131.

37. Dunning, W.J., "General and Theoretical Introduction (to Nucleation)" Chapter in Nucleation, A.C. Zettlemoyer, ed. Marcel Dekker, N.Y. (1969).

38. Eckstein, B., "Vitreous States," Mat. Res. Bull. 3 199-208 (1968).

39. Ewing, R.H., "The Free Energy of the Crystal-Melt Interface From the Radial Distribution Function," J. Cryst. Growth 11 221 (1971).

40. Fisher, J.C., et. al. "Nucleation," J. Appl. Phys. 19 775 (August 1948).

41. Frank, F.C., "An Outline of Nucleation Theory," J. Cryst. Growth. 13/14 154 (1972).

42. Ghez, R., "An Exact Calculation of Crystal Growth Rates Under Conditions of Constant Cooling Rate," J. Cryst. Growth 19 153 (1973).

BIBLIOGRAPHY (CONT'D)

43. Ghez, R. and Lew, J.S., "Interface Kinetics and Crystal Growth Under Conditions of Constant Cooling Rate," J. Cryst. Growth 20 273 (1973).

44. Gibbs, J.H., "Nature of the Glass Transition and the Vitreous State," in Modern Aspects of the Vitreous State, I, J.D. Mackenzie, ed.

45. Gilmer, G.H. and Bennema, P., "Computer Simulation of Crystal Surface Structure and Growth Kinetics," J. Cryst. Growth 13/14 148 (1972).

46. Gutzow, I. and Kashchiev, D., "Kinetics of Overall Crystallization of Undercooled Melts in Terms of the Non-Steady State Theory of Nucleation" in Adv. Nucleation and Crystallization in Glasses, L.L. Hench and S.W. Frieman, eds., Am. Ceram. Soc. Sp. Publ. #5 (1971).

47. Hammel, J.J., "Direct Measurements of Homogeneous Nucleation Rates in a Glass-Forming Systems," J. Chem. Phys. 46 (6) 2234 (1966).

48. Heaton, H.M. and Moore, H., "A Study of Glasses Consisting Mainly of the Oxides of Elements of High Atomic Weight, Part III. The Factors Which Determine the Possibility of Glass Formation," J. Soc. Glass Technol. XLI (198) Feb. 1957.

49. Hillig, W.B., "Kinetics of Solidification from Nonmetallic Liquids" in Kinetics of High Temperature Processes, W.D. Kingery, ed.

50. Hillig, W.B. and Turnbull, D., "Theory of Crystal Growth in Undercooled Pure Liquids," J. Chem. Phys. 24 (4) 914 (1956).

51. Hopper, R.W., et. al., "Crystallization Statistics, Thermal History, and Glass Formation," J. Non-Cryst. Solids. 15 45-62 (1974).

52. Hopper, R.W. and Uhlmann, D.R., "Solute Redistribution During Crystallization at Constant Velocity and Constant Temperature." J. Cryst. Growth. 21 203 (1974).

53. Hopper, R.W. and Uhlmann, D.R., "Temperature Distributions During Crystallization at Constant Velocity," J. Cryst. Growth 19 177 (1973)

54. Jackson, K.A., "On Surface Free Energy Calculations," J. Cryst. Growth 10 119 (1971).

BIBLIOGRAPHY (CONT'D)

55. Jones, D.R.H., "A Mechanical Model of Solid-Liquid Interfaces" J. Cryst. Growth 21 167 (1974).

56. Knight, C.A., "Breeding of Crystal Nuclei by Classical Nucleation: Theory and Some Observations and Experiments." J. Cryst. Growth, 11 201 (1971).

57. Konak, A.R., "Difficulties Associated with Theories of Growth from Solution." J. Cryst. Growth 19 247 (1973).

58. Lothe, J. and Pound, G.M., "Statistical Mechanics of Nucleation" Chapter in Nucleation, A.C. Zettlemoyer, ed., Marcel Dekker, N.Y. (1969).

59. MacDowell, J.F., "Nucleation in Glasses," in Nucleation Phenomena, Am. Chem. Soc. (1966).

60. Magill, J.H. and Li, H.M., "A Corresponding States Equation for Crystallization Kinetics," J. Cryst. Growth 19 361 (1973).

61. Markov, I. and Kashchiev, D., "Nucleation on Active Centres 1. General Theory," J. Cryst. Growth 16 170 (1972).

62. McMillan, P.W., Glass-Ceramics, Chapter 2, "Crystallization and Devitrification," Academic Press, N.Y. (1964).

63. Robertson, D. and Pound, G.M., "Numerical Simulation of Heterogeneous Nucleation and Growth," J. Cryst. Growth. 19 269 (1973).

64. Sarjeant, P. and Roy, R., "New Approach to the Prediction of Glass Formation," Mat. Res. Bull. 3 265-80 (1968).

65. Sears, G.W., "Recent Developments in Nucleation Theory," in Physics and Chemistry of Ceramics, C. Klingsberg, ed., Gordon and Breach, 1963.

66. Stevels, J.M., "Permitted and Forbidden Structural Units in Vitreous Systems," Mat. Res. Bull. 3 599-610 (1968).

67. Sun, K., "Fundamental Condition of Glass Formation," J. Am. Ceram. Soc. 30 (9) 277 (1947).

68. Tashiro, M., "Nucleation and Crystal Growth in Glasses," Eighth International Congress on Glass, 1968.

69. Turnbull, D., "Phase Charges" in Solid State Physics - Advances in Research and Applications, Vol. 3, Academic Press, N.Y. (1956).

70. Turnbull, D., "Inc. What Conditions Can a Glass be Formed?" Contemp. Phys. 10 (5) 473-88 (1969).

BIBLIOGRAPHY (CONT'D)

71. Turnbull, D. and Cohen, M.H., "Free-Volume Model of the Amorphous Phase: Glass Transition," J. Chem. Phys. 34 (1) 120 (1961)

72. Walton, A.G., "Nucleation in Liquids and Solutions," Chapter in Nucleation, A.C. Zettlemoyer, ed.,Marcel Dekker, N.Y. (1969)

73. Walton, A.G., "Bulk and Surface Transport in Liquids - An Introductory Treatment," Contemp. Phys. 10 (5) 489 (1969)

74. White, W.B. and Berkes, J.S., "Calculation of Volume Free Energy of Nucleation of a Crystalline Phase from a Multi-component Regular Solution," J. Am. Ceram. Soc. 52 (4), 231, 1969.